doi.org/10.1002/batt.202000264

Special Collection

Recent Advances on Carbon-Based Materials for High Performance Lithium-Ion Capacitors

Wenjie Liu,[a, b] Xiong Zhang,*[a, b, e] Yanan Xu,[a] Chen Li,[a] Kai Wang,[a, b, e] Xianzhong Sun,[a] Fangyuan Su,[c, e] Cheng-Meng Chen,[c, e] Fangyan Liu,[d, e] Zhong-Shuai Wu,[d, e] and Yanwei Ma*[a, b]

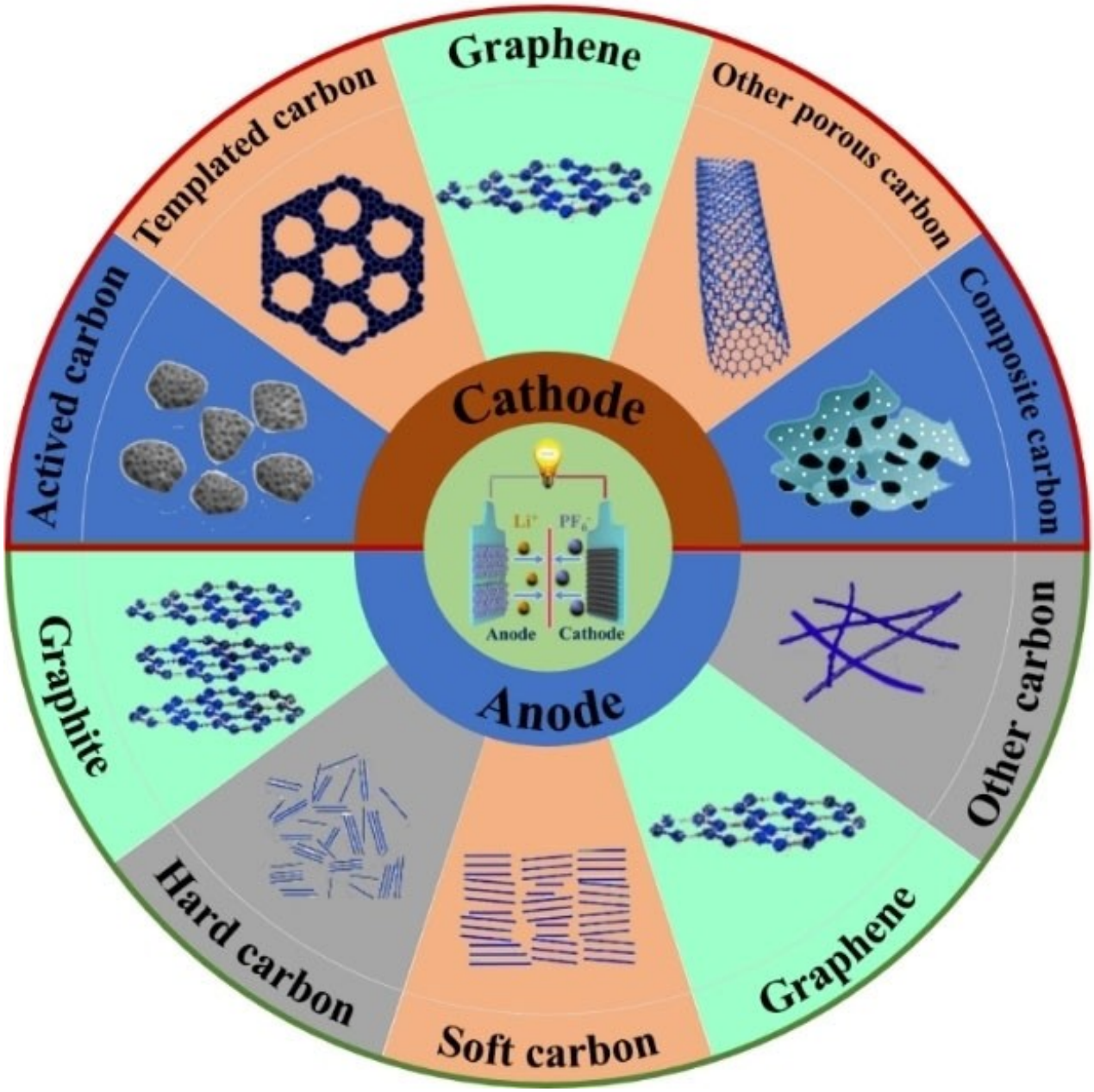

doi.org/10.1002/batt.202000264

Lithium-ion capacitors (LICs) combining of lithium-ion batteries (LIBs) and supercapacitors (SCs) with improved performance bridge the gap between these two devices, and have attracted huge attention in the field of high-efficiency electrochemical energy storage. The behavior of electrode materials is essential for the realization of high energy and high output LICs devices. As the most widely utilized electrodes, carbon materials demonstrated their ability in LICs with fast charge storage and long life-span. Here, an overview of carbon materials for advanced LICs applications is given. The advantages and shortcomings of carbon materials as electrodes are systematically analyzed with the purpose of disclosing their influence on LICs devices. In light of this analysis, the critical aspects are discussed, which should be dealt with in the future for the realization of desires high-performance LICs devices.

1. Introduction

Sustainable energy development strategies are urgently needed to meet the demands of contemporary social development without jeopardizing future generations and also satisfy their energy needs.[1–3] For achieving the efficient utilization and storage of sustainable energy, an advanced energy device is extremely important. Among various energy storage devices, electrochemical energy storage (EES) devices meet this requirement well and have been developed rapidly in recent decades.[4–7] At present, lithium-ion batteries (LIBs) and supercapacitors (SCs) are the most commonly used EES devices in social daily life. The energy density of state-of-the-art LIBs is about 150 ~ 300 Wh/kg, with limited power density (less than 2 kW/kg) and short cycle life (~ 1000 cycles).[8–12] By contrast, SCs usually possess high power density (> 10 kW/kg) and long life-span (~ 10^5 cycles) but poor energy density (< 10 Wh/kg).[13–16] However, driven by the expansion of the markets for electric vehicles, mobile intelligent electronic productions, and auxiliary energy storage (for intermittent photovoltaic or wind power sources),[17] the requirements for advanced EES devices are getting higher and higher. Considering the significant defects of LIBs and SCs, new prototype EES devices that can simultaneously achieve high energy density, high power density, and prolonged cycle life are clear required for their further application in the electronic market.[18–20]

In 2001, a lithium-ion capacitor was firstly reported by Amatucci et al.[21] with activated carbon (AC) as cathode and $Li_4Ti_5O_{12}$ (LTO) as the anode in an organic electrolyte, which delivered an energy density of 20 Wh/kg (based on the packaged device). Subsequently, various prototypes of LICs emerged and their electrochemical performances were continuously enhanced.[22–25] The advent of LICs makes up the huge gap between the performance of LIBs and SCs. As shown in Figure 1a, the energy and power density of LICs lie in between those of LIBs and SCs, which is significantly dependent on the charge storage mechanism.[26] In general, LICs are constructed by a capacitor-type cathode coupled with a pre-lithiated battery-type anode in an appropriate Li-salts-containing electrolyte.[27–28] Simply, a non-Faradaic reaction (rapid ions absorption/desorption) occurs on the capacitor-type electrode/electrolyte interface and is usually accompanied by a linear change of electrode voltage.[29–31] Meanwhile, a pre-lithiated battery-type electrode undergoes a Faradaic reaction (sluggish Li^+ insertion/extraction process) at a relatively stable potential.[32–34] Furthermore, LICs have a wider operating voltage window than SCs and LIBs, so the energy density has been improved accordantly (Figure 1b).[35] However, it is generally known that the capacitor-type cathode delivers a much lower specific capacity compared to the battery-type anode. Thus, the existence of two distinct working mechanisms in LICs raises the issue of capacity and kinetics matching. According to the "barrel principle", the energy density of the whole LIC device is determined by the capacitor-type electrode, and the power density and cycle life are mainly affected by the battery-type electrode.[36–37] For the sake of expanding the commercial use of LICs, the aforementioned problems should be solved to enhance the performance of LIC devices. To achieve this goal, it is essential to select and realize advanced electrode materials.

The electrode materials play a crucial role in the electrochemical performance of LICs.[38] For the capacitor-type electrode, the rapid charge-discharge ability and cyclic stability are its remarkable characteristics. Just like the requirements of electrode materials for SCs, the capacitor-type materials need to possess a high specific surface area (> 1000 m^2/g), high intrinsic conductivity, and sufficient contact surface area with electrolyte.[39] Carbonaceous materials (AC, graphene, CNT, etc.) and pseudo-capacitive active materials (metal oxide or nitride, and conducting polymers) are the main capacitor-type materi-

[a] W. Liu, Prof. X. Zhang, Dr. Y. Xu, Dr. C. Li, Prof. K. Wang, Dr. X. Sun, Prof. Y. Ma
Institute of Electrical Engineering
Chinese Academy of Sciences
Beijing 100190, China
E-mail: zhangxiong@mail.iee.ac.cn
ywma@mail.iee.ac.cn
[b] W. Liu, Prof. X. Zhang, Prof. K. Wang, Prof. Y. Ma
School of Engineering Sciences
University of Chinese Academy of Sciences
Beijing 100049, China
[c] Dr. F. Su, Prof. C.-M. Chen
CAS Key Laboratory of Carbon Materials, Institute of Coal Chemistry
Chinese Academy of Sciences
Taiyuan 030001, Shanxi, China
[d] Dr. F. Liu, Prof. Z.-S. Wu
State Key Laboratory of Catalysis, Dalian Institute of Chemical Physics
Chinese Academy of Sciences
Dalian 116023, China
[e] Prof. X. Zhang, Prof. K. Wang, Dr. F. Su, Prof. C.-M. Chen, Dr. F. Liu, Prof. Z.-S. Wu
Dalian National Laboratory for Clean Energy
Chinese Academy of Sciences
Dalian 116023, China
Special Collection An invited contribution to a Special Collection dedicated to Metal-Ion Hybrid Supercapacitors.

doi.org/10.1002/batt.202000264

Wenjie Liu completed his Master's Degree study in polymer chemistry and physics at Nanjing University of Science and Technology (NUST) in 2018. He is currently pursuing a Ph.D. degree at the Institute of Electrical Engineering, Chinese Academy of Sciences (CAS), under the supervision of Prof. Xiong Zhang. His research focuses on graphene-based high-performance lithium-ion capacitors.

Prof. Xiong Zhang received his B.S. in applied chemistry from Central South University in 2003, and his Ph.D. in applied chemistry from Beijing University of Chemical Technology in 2008. Then he joined the Institute of Electrical Engineering, Chinese Academy of Sciences. His research interests focus on the synthesis of electrode materials for supercapacitors and the applications of lithium-ion capacitors.

Dr. Yanan Xu received his Ph.D. degree in the Department of Materials Science of Engineering from the Wuhan University of Technology in 2019. Then he joined the Institute of Electrical Engineering, Chinese Academy of Science, as a research assistant. His current research involves the nanomaterials achieving high energy density and power density for the electrochemical energy storage device.

Dr. Chen Li completed his B.S. study in polymer materials and engineering at Beijing University of Chemical Technology (BUCT) in 2010 and obtained his Ph.D. degree in electrical engineering from the University of Chinese Academy of Sciences (UCAS) in 2017. In the same year, he joined the Institute of Electrical Engineering (IEE), Chinese Academy of Sciences (CAS). His research interests focus on the design and fabrication of advanced carbon-based energy materials for high-performance supercapacitors and lithium-ion capacitors.

Prof. Kai Wang received his B.S. from the Department of Chemistry and Chemical Engineering of Shandong University (2007), and his Ph.D. from National Center for Nanoscience and Technology (NCNST). After a postdoctoral experience in Singapore-MIT Alliance for Research and Technology (SMART), he joined the Institute of Electrical Engineering, Chinese Academy of Science in 2014. His current research interests are in the field of electrochemical energy materials and devices, with a focus on hybrid nanomaterials, supercapacitors, and solid-state lithium-ion batteries.

Dr. Xianzhong Sun received his Bachelor's Degree from the Department of Mechanical Engineering of Wuhan Institute of Technology (1999), Master Degree from Department of Materials Science & Engineering of Zhejiang University (2006), Doctoral Degree from Department of Materials Science & Engineering of Tsinghua University (2011). He joined the Institute of Electrical Engineering, Chinese Academy of Sciences (IEE CAS) in 2011. His current research interests are in the fields of novel electrochemical energy storage devices, including electrical double-layer capacitors, lithium-ion capacitors (LIC), and lithium-ion battery type capacitors (LIBCs).

Dr. Fangyuan Su received his Ph.D. in Applied Chemistry (Electrochemistry) from Tianjin University in 2012, and worked as a postdoc at Tsinghua University in 2012–2014. Then he joined the Institute of Coal Chemistry, CAS in 2014, and now works as an associate professor. He has published about 40 research articles. His research focuses on the design and simulation of electrochemical energy storage devices including supercapacitor, Li-ion battery, and Li-S battery.

Prof. Cheng-Meng Chen serves as deputy director of CAS Key Laboratory of Carbon Materials, and principal investigator of Group 709 at Institute of Coal Chemistry, Chinese Academy of Sciences (ICC, CAS). He is dedicated to research and development of advanced carbon materials and their applications in energy storage devices. He won the first prize of Natural Science Award of Shanxi Province, and Hou Debang Youth Award of Chemical Engineering Technology, etc. Prof. Chen was selected as the MIT Technology Review 2017 innovator under 35 in China and got the foundation of Outstanding Youth Fund by National Natural Science Foundation of China in 2019.

Dr. Fangyan Liu received her Ph.D. from Northeast Forestry University in 2015. She worked as a postdoc focused on high-energy supercapacitors in Southwest Jiaotong University in 2015–2019, and continued to conduct postdoctoral research for high-energy energy storage devices at Dalian Institute of Chemical Physics, CAS until now. Her research interests mainly concentrate on 2D materials for high-energy supercapacitors and Li-ion capacitors.

Prof. Zhong-Shuai Wu obtained his Ph.D. from the Institute for Metal Research, CAS in 2011 and worked as a postdoctoral fellow at the Max Planck Institute for Polymer Research in Mainz, Germany from 2011 to 2015. Then, he became a full Professor and Group Leader of 2D Materials & Energy Devices at DICP, CAS, and was promoted in 2018 as a DICP Chair Professor. Currently, Prof. Wu's research interests include graphene and 2D materials, surface- and nanoelectrochemistry, microscale electrochemical energy storage devices, supercapacitors, batteries and catalysis.

Prof. Yanwei Ma obtained his Ph.D. degree from Tsinghua University in 1996 and then worked as a post-doctoral fellow at the University of Science and Technology Beijing (USTB). Following research associate positions at Institute for Materials Research, Tohoku University (Sendai, Japan), National Institute for Materials Science (Tsukuba, Japan), and Université de Rennes 1 (France), he joined the Institute of Electrical Engineering, Chinese Academy of Sciences in 2004 as a full-time professor. He leads a team focused on superconductivity and new energy materials. His research activities are devoted to the development of superconducting wires and nanomaterials for energy storage, and fabrication of graphene-based supercapacitors.

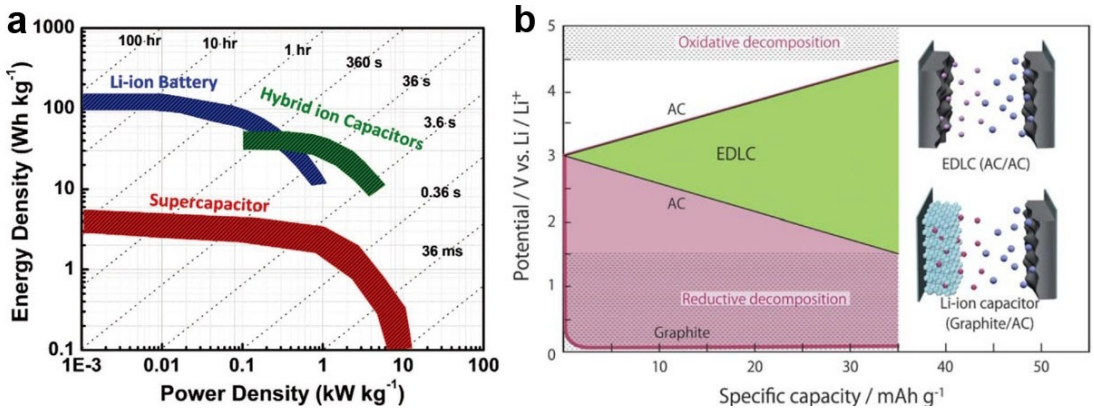

Figure 1. a) Ragone plots of various energy-storage devices. Reproduced from Ref. [26] with permission. Copyright (2020) The Authors. b) Typical voltage curves and charge storage mechanism for an EDLC and a LIC device, respectively. Reproduced from Ref. [35] with permission. Copyright (2012) The Royal Society of Chemistry.

als for LICs cathode.[40–42] For the battery-type electrode of LICs, the materials can be divided into three kinds according to their various Li^+ storage behavior: insertion-type of pre-lithiated carbonaceous materials (graphite, hard carbon, and soft carbon, etc.), TiO_2,[43–44] and LTO;[45] conversion-type of metal oxides and hydroxides materials (SnO_2,[46–47] Fe_3O_4,[48] Nb_2O_5,[49–50] CoO,[51] etc.), and alloy-type metal or metallic compounds (Si,[23,52] Sn,[53–54] etc.). However, although nearly thousands of materials have been developed for LICs cathode or anode in recent years, only a few of them are viable for commercial application due to the inferior capacity, or high cost, poor structural stability, and so on.

Considering that high energy density and rapid charging ability are important for various commercial electronic equipment (like battery electric vehicles), the property of long cycle life, low production cost, and high security for LICs are also critical.[55–56] Hence, although the theoretical capacity of the carbonaceous electrode cannot catch up with some novel-type reported electrode materials, carbon materials possess the characteristics of non-poisonous, high electrical conductivity, low-cost, the abundance of raw materials, renewability, controllable high specific surface area, and stable physicochemical properties.[57–60] So that they can be used as suitable electrode materials to satisfy the above requirements of LIC devices. Taking this into account, carbon materials as electrode materials for LICs have moved from laboratory research to the road of industrial production and have made good progress.[61] However, carbon materials still have some challenges that demand to be addressed, such as coulombic efficiency (CE), capacity, and energy density. Through researching carbon materials as LICs cathode, acquiring a high specific surface area and a suitable pore-size distribution design are effective ways to improve the energy storage capacity of electric double layer carbon-based materials. Introducing heteroatom doping or function groups to provide pseudo-capacitance is also viable.[27,62] In the case of carbon materials as LICs anode, the main purpose of the research is devoted to improving the Li^+ diffusion kinetics in the bulk materials and cycling stability. By appropriately controlling the microscopic morphology and delicate structure design, the conductivity and structure stability of carbon materials can be improved, therefore, the electrochemical performance of carbon-based LICs can be enhanced.[63–64]

Currently, a certain number of special reviews on LICs have been published. Li et al.[65] described in detail the latest development of graphene-based materials applied in LICs. Su et al.[66] proposed the challenges and opportunities of 2D materials in advanced lithium-ion capacitors. Li et al.[27] reviewed the recent progress of electrode materials in LICs, along with the development and design requirements of electrolytes. Besides, some related reviews about EES systems have also mentioned the progress of LICs. However, so far, no systematic review of carbon-based materials as electrodes for advanced LICs has been reported. Herein, a comprehensive summarization of carbon-based materials for LICs application is proposed, either as a cathode or anode material. Also, the prospects and key issues related to the development of carbon-based LICs are discussed. Finally, an outlook about developing appropriate materials and solving the vital problems for the realization of advanced LICs will be identified.

2. Carbonaceous as Cathode Materials in LICs

Capacitor-type materials are the most common selection of cathode for high power and long cycle life LICs devices. At present, carbonaceous materials are the most widely utilized materials for the commercial EES market, which is relying on its fast physical ion adsorption/desorption storage process and high working voltage.[59] According to the different synthesis methods and physicochemical properties, carbonaceous materials can be divided into AC, templated carbons (TCs), graphene, and so on.

doi.org/10.1002/batt.202000264

2.1. Activated Carbon

As the most typical capacitor-type materials, low-cost AC plays an important role in the application of LICs. Usually, AC can be easily produced by carbonizing biomass materials, petroleum coke, or polymer precursors at 600 ~ 900 °C.[58] However, the AC prepared above usually has an unsatisfactory capacity due to its low specific surface area and low electronic conductivity. Hence, a physical or chemical etching activation process is normally needed.[13] Examples include gentle physical etching in CO_2, water vapor or mixed steam atmosphere, or chemical etching with a strong oxidant such as KOH, $ZnCl_2$, and HNO_3.[67–68] Therefore, AC has the characteristics of a large specific surface area (1000 ~ 2000 m^2/g), high porosity (most of the holes are micropores), and exist a certain amount of functional groups in the structure. The electric double-layer capacitance of AC ensuring the high power output and long life span of LICs devices. Jain et al.[69] prepared a high mesoporosity AC (Figure 2a) by hydrothermal and chemical/physical activation treatment of coconut shells. The prepared carbon cathode (ZHTP) delivered a superior capacity than commercial activated carbon (CAC), as shown in Figure 2b. Then, the tailored AC was employed as the cathode and commercial LTO as the anode to fabricate a LIC. The obtained LIC device exhibited a high energy density of 69 Wh/kg (based on the whole active materials mass of cathode and anode, the followings are calculated in the same way if not specified), and 2000 cycles with a capacity retention of 85 %, which is attributed to the high mesoporosity of AC and the good structural stability of electrode materials. Dsoke et al.[70] proposed a simple way to reduce the diffusion resistance and polarization of the electrode by modulating the mass ratio of AC/LTO materials, the optimized LIC delivered an improved energy density and cycle life.

However, AC is generally amorphous and has relatively low electronic conductivity (about tens of S/cm) due to the low temperature of carbonization and activation processes. Besides, part of the pores cannot be utilized, resulting in an insufficient effective surface area, so the actual capacity of AC is low.[73–74] Heteroatoms doping is an effective way to enhance the performance of AC by increasing the electrical conductivity and providing additional active sites.[75] A suitable biomass precursor material (corncob) was selected by Li et al.[71] to in-situ synthesize a nitrogen-doped ACs (NACs) with a controllable

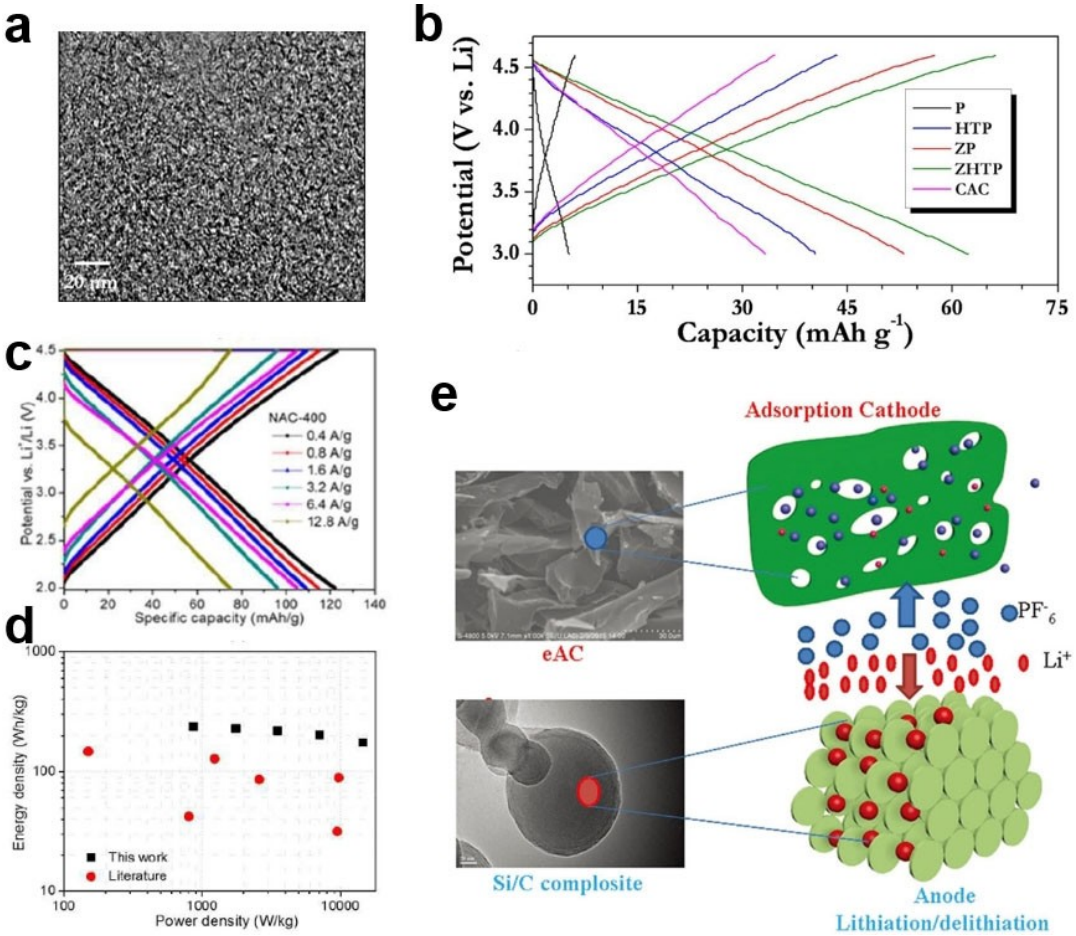

Figure 2. a) Field emission transmission electron microscopy (FE-TEM) images of ZHTP and (b) charge-discharge profiles of various carbon cathode materials in a half-cell. Reproduced from Ref. [69] with permission. Copyright (2013) The Authors. c) Voltage profile of NAC-400 at different current densities and d) Ragone plot of the NAC-400-Si/C LIC. Reproduced from Ref. [71] with permission. Copyright (2016) The Royal Society of Chemistry. e) The eAC anode and Si/C cathode materials for LIC device and schematic diagram of charge storage. Reproduced from Ref. [72] with permission. Copyright (2016) Wiley-VCH.

pore structure. The N-doping can not only increase the electronic conductivity but also improve the capacity of AC via introducing the pseudocapacitance. Benefited from the concentrated micro-/meso-porous distribution and appropriate N content, the NACs achieved a high specific capacity of 129 mAh/g (Figure 2c). The LIC assembled by NACs and Si/C electrode delivered an energy density up to 230 Wh/kg at a power density of 1747 W/kg, the energy density could still maintain 141 Wh/kg when the power density reached 30127 W/kg (Figure 2d). The cycling stability of obtained LICs was well with about 23.7% capacity decay after 8000 cycles. Furthermore, activation temperature also has a great influence on the performance of activated carbon. The same group[72] also proved a high specific surface area AC derived from egg white (eAC) could be easily applied to large-scale production (Figure 2e). By adjusting the activation temperature, the degree of graphitization, and the content of the surface oxygen functional group changed accordantly, which could affect the wettability and the charge transfer rate on the AC surface. The advanced LIC based on the obtained eAC showed an energy density of 257 Wh/kg and a power density of 29893 W/kg with a prolonged life span of 79.2% capacity retained after 15000 cycles, much higher than that reported in the literature. Besides, AC materials derived from sisal fibers[76] or Chinese-chive[77] as carbon precursors have also revealed good electrochemical properties in LICs. From the above, controlling the heating-treatment temperature, fine-tuning pore structure, and heteroatom doping are effective ways to improve the performance of AC. However, obtaining the AC with a high specific surface area is often at the expense of the density of the material, thus materials with low tap density will further affect the volume energy density of the whole devices. Mechanical stability designs and internal densification are both available solutions for the realization of AC cathode materials with high gravimetric and volumetric performance.

2.2. Templated Carbon

Although AC possesses a high specific surface area, most of the specific surface area is provided by micropores, and the random pore size distribution will lead to high pore tortuosity and abundance of blind or dead micropores, resulting in insufficient contact with solvated ion and limited capacity utilization.[78] For the purpose of increasing the carbon cathode capacity and reducing its capacity disparity compared with the battery-type anode material, the novel carbon materials with a suitable pore size distribution from micro- to meso-pores are essential. To acquire a carbon material with a desirable pore structure, a template-assisted method can be used by carbonizing the carbon precursor and removing the template subsequently. The obtained porous carbons are called template carbons, and the pore size is accurately controlled in the mesoporous range usually. The mesopores have a great influence on the fast ion transportability of carbon materials electrodes.[79] The templates utilized to tune the pore size of TCs can be divided into two types.[80] One is hard-template, including zeolites,[81] metal oxide/chloride, and mesoporous silica spheres (MSS). The other is soft-template such as polystyrene microsphere and metal-organic framework (MOF). Each template has its distinctive feature, and the corresponding TCs have been widely applied as cathode for high energy and power LIC devices in recent years.

The hard-template method usually requires the template to be easily removed in the subsequent processing. Therefore, the selection of an appropriate template is critical. NaCl is an ideal hard template, which can be easily removed by water to obtain porous carbon. Shi's group[82] prepared a hierarchical porous carbon (EM-NaCl) by using egg white as a biomass carbon precursor mixed with a template of NaCl, as shown in Figure 3a. The NaCl could not only be used as a template for generating macropores (>50 nm), but also as a graphitization catalyst to increase the degree of graphitization. As a result, the activated EM-NaCl (a-EW-NaCl) achieved a high specific capacity of 118 mAh/g. Furthermore, the LIC assembled by the a-EW-NaCl cathode and Fe_3O_4@C anode delivered an energy density of 124.7 Wh/kg and a power density of 16989 W/kg with a stable cyclability (88.3% capacity retention after 2000 cycles). Song's group[83] synthesized a hierarchical porous carbon (HPC) by using asphalt and porous MgO as a carbon precursor and template, respectively. The obtained HPC possessed distinct mesopores with a concentrated pore size of ~4.06 nm (Figure 3b) and meanwhile accompanied by abundant micropores (derived from KOH activation). Subsequently, the HPC was used as both cathode and anode material to assemble a LIC, and the device exhibited an energy density of 189 Wh/kg, a power density of 14431 W/kg, and excellent capacity retention of 91.3% after 10000 cycles (Figure 3c). Similarly, Cheng et al.[84] reported a hierarchical porous N-doped carbon through carbonizing polydopamine with the assistance of MSS (~50 nm) hard template. Then, a high-performance LIC was fabricated based on the obtained carbon materials, which showed high energy densities of 145–57.5 Wh/kg at power densities from 1.4 to 17.3 kW/kg and 5000 cycles with retention of 85%.

As for the soft-template method, the template material is generally removed directly during the high-temperature heat-treatment process. Hence, the soft-template method is more convenient than the hard-template, but the selection of an appropriate soft-template for the desired carbon materials is more challenging. At present, MOF, Zeolite imidazole frameworks (ZIFs), and MSS are the common soft-template materials that are used in synthesizing porous carbon as a cathode in LIC devices. For example, MOF-derived high surface area carbon material (MOF-DC) with a high concentration of micropores (~0.5 nm) was presented by Banerjee's group,[85] as shown in Figure 3d. In this study, benefited from the high surface area (2714 m^2/g) and hierarchical porous morphology of MOF-DC as the cathode, the fabricated LIC device (LTO as the anode) realized an energy density of 65 Wh/kg as well as long cycling performance with ~82% retention after 10000 cycles. Recently, Zou et al.[86] synthesized a porous carbon by using Zeolite imidazole frameworks (ZIFs) as both template and carbon precursors. The enhanced graphitization degree and a suitable

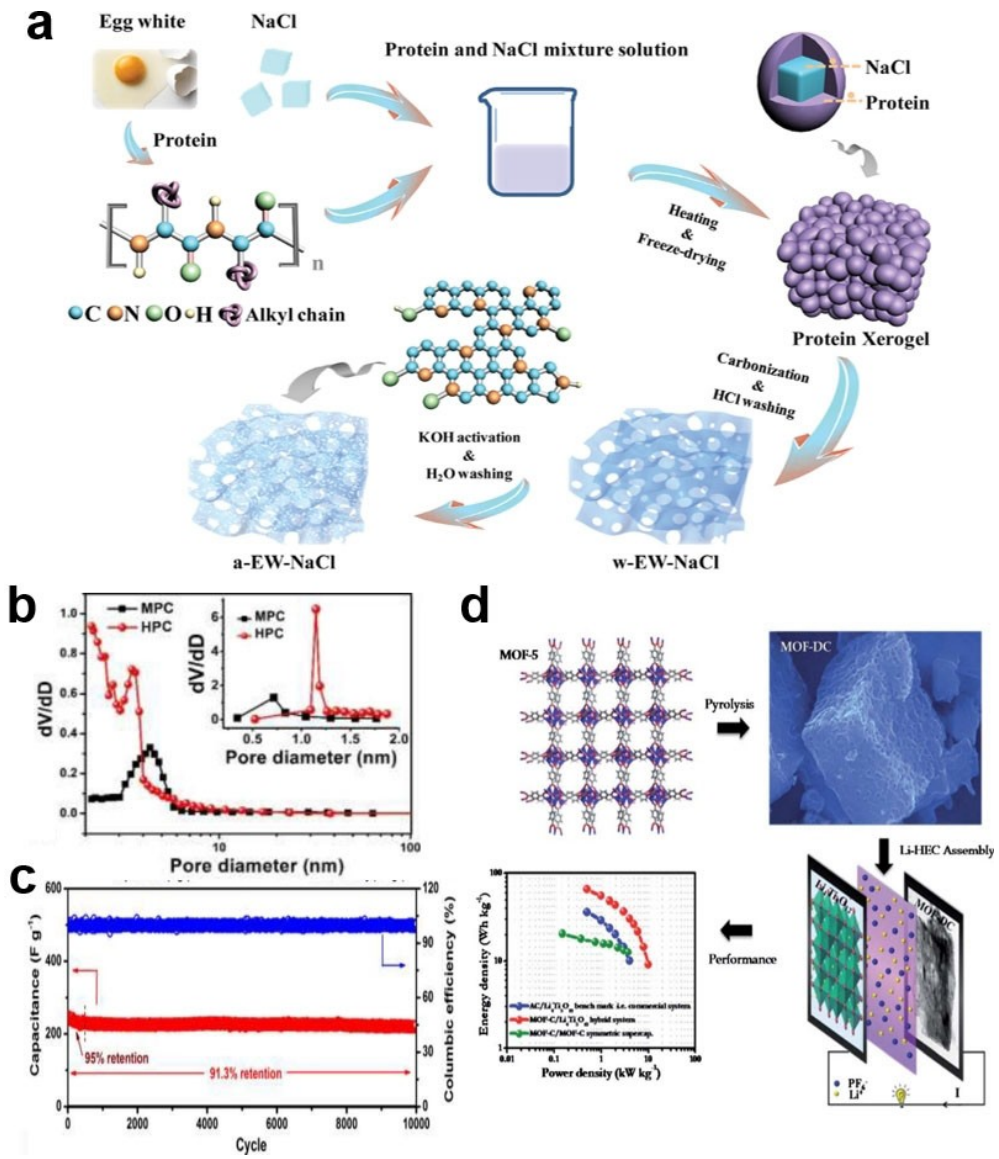

Figure 3. a) Schematic chart for the preparation of a-EW-NaCl. Reproduced from Ref. [82] with permission. Copyright (2018) The Royal Society of Chemistry. b) PSD of HPC materials and c) cycle stability of HPC//HPC LIC device. Reproduced from Ref. [83] with permission. Copyright (2018) Wiley-VCH. d) Synthesis of MOF-DC and its application for LIC. Reproduced from Ref. [85] with permission. Copyright (2014) The Royal Society of Chemistry.

pore size distribution (1.5–3 nm) improved the capacity and rate performance of the obtained carbon materials. Therefore, the porous carbon was used as a cathode, and together with a pre-lithiated graphite (PLG) anode for preparing a LIC. A high energy and power density of the device could achieve 108 Wh/kg and 15 kW/kg, respectively. Excellent cycling stability was also presented with 10000 cycles in 2–4 V.

Overall, TC materials with a controlled and uniform pore distribution and nanostructure have inspired interest in its application for LIC devices. And the capacity and cycling performance of TCs as LIC cathodes have been further enhanced. However, the introduction of templates increases production costs and the process is more complicated, so its commercial development is limited. A facile and low-cost method to synthesize high-performance porous carbon materials is a significant research field in the future.

2.3. Graphene

As a typical two-dimension (2D) material, graphene is commonly composed of an atomically thin carbon layer in a hexagonal lattice form. So far, many approaches have been reported for synthesizing graphene with various properties, and these methods can be divided into two categories: one is the "top-down" approach, such as exfoliating graphite by liquid-phase or high-energy shearing treatment to obtain graphene oxide (GO), and then the reduction of GO; the other is "bottom-up" synthesis of graphene by chemical vapor deposition (CVD), epitaxial growth or advanced organic chemistry approach.[87–88] Compared with AC, graphene has a high specific surface area (~2630 m^2/g, theoretically), high intrinsic capacitance, and relatively high internal electronic conductivity.[89–91] However, much of these excellent properties

are usually realized in mono- or fewer-layer graphene.[92] The inevitable aggregation and overlaying of the graphene sheet cause the bulk-graphene with a graphite-like structure, which severely reduced their effective ion-contact surface by at least two orders of magnitude.[93] As a result, for the sake of improving the properties of graphene as a LIC cathode, the introduction of functional groups on the surface of graphene or pre-insertion of nano-materials between the graphene layers as pillars is a very promising mean to solve the restacking of graphene.[94–95] Besides, fabricating a three-dimensional (3D) hierarchical structure based on 2D graphene layer can radically ameliorate the self-restacking impact by controlling the space organization structure.[96–97]

In a previous study, Lee et al.[98] prepared functionalized graphene with a grass-like structure via the assistance of urea reduction (URGO, Figure 4a). The amide functional group was introduced in the urea reduction process, which could promote the reversible combination with lithium-ion by the enolization process. Thus the specific capacity of amide-functionalized URGO (35 mAh/g) was 35% higher than that of AC (26 mAh/g). Moreover, the LIC assembled by a PLG anode and a URGO cathode provided high energy densities of 106–85 Wh/kg with power densities range of 84–4200 W/kg, as well as good cycle stability up to 1000 cycles. Similarly, aiming to improve the capacity and cycling performance of graphene, an eco-friendly trigol was used by Aravindan's group[99] to reduce GO (TRGO). Benefited from the PF_6^- anion fast adsorption/desorption ability, the reversible capacity of TRGO could increase to 58 mAh/g (Figure 4b). A LIC device based on a TRGO cathode and a LTO anode delivered high energy of 45 Wh/kg with a high power density of 3.3 kW/kg, and prolong cycling ability for 5000 cycles. Moreover, the diffusion rate of electrolyte ions across the graphene basal plane can be significantly increased by adjusting the in-plain pore of graphene, thus enhancing the capacity and rate performance of the electrode. Stoller et al.[100] reported a KOH activated microwave expanded graphite oxide (a-MEGO) as cathode and graphite as anode for preparing LIC devices. The high specific surface area of a-MEGO with a hierarchical pore structure (ranges from <1 to 10 nm) demonstrated a high capacity of 125 mAh/g. The integrated LIC realized an energy density of 147.8 Wh/kg in the tetraethylammonium tetrafluoroborate/acetonitrile ($TEABF_4$/AN) electrolyte. A later study by Mhamane et al.[101] reported a macro-graphene-like porous carbon (>500 nm) with a high-level of sp^2 hybridization through a simple bottom-up method, which could deliver a high discharge capacity of about 74 mAh/g

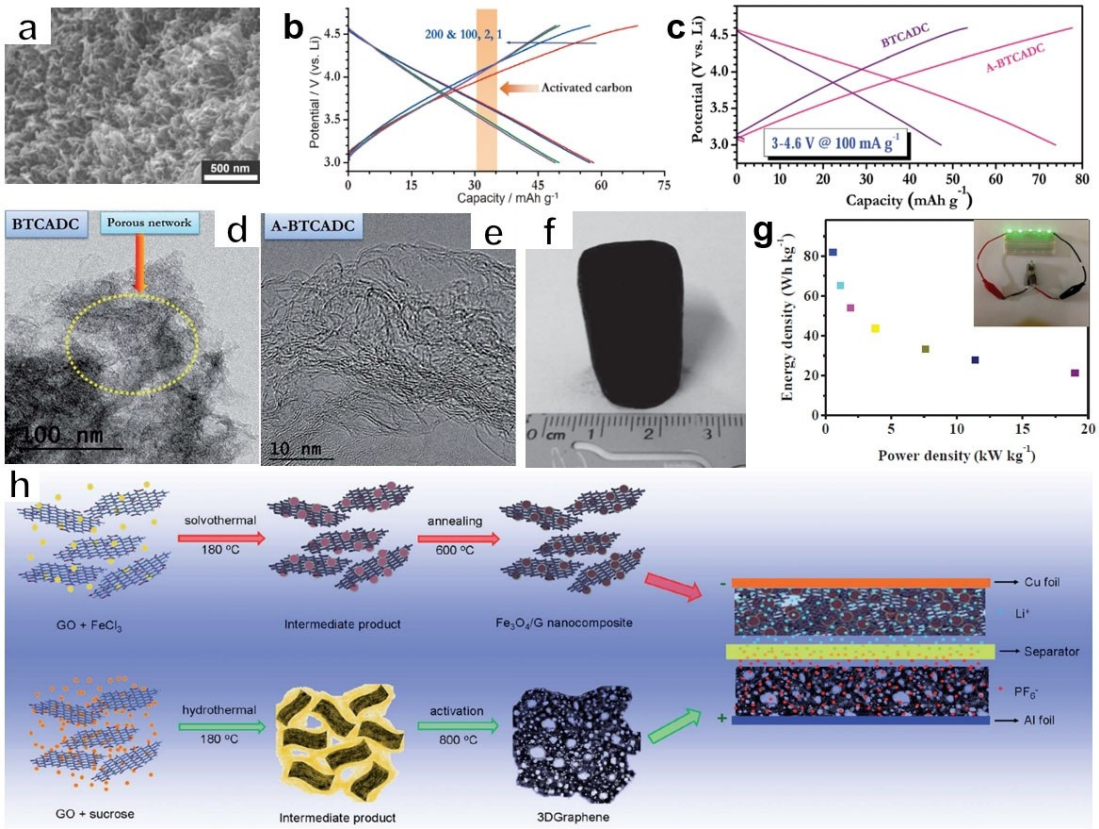

Figure 4. a) A scanning electron microscopy (SEM) picture of URGO. Reproduced from Ref. [98] with permission. Copyright (2012) Wiley-VCH. b) The galvanostatic current charge-discharge curves of TRGO in a half-cell configuration vs. Li foil. Reproduced from Ref. [99] with permission. Copyright (2013) Wiley-VCH. c) The comparison of constant current charge-discharge curves for BTCADC and A-BTCADC electrodes in a Li half-cell. High-resolution transmission electron microscopy (HR-TEM) pictures of d) BTCADC and e) A-BTCADC. Reproduced from Ref. [101] with permission. Copyright (2016) The Royal Society of Chemistry. f) Photograph of the graphene hydrogel. g) Ragone plots of NBAs//Graphene hydrogels LIC devices. Reproduced from Ref. [102] with permission. Copyright (2014) Wiley-VCH. h) Schematic diagram of synthesizing the Fe_3O_4/G cathode and the 3D Graphene anode, together for the final fabrication of the LIC device. Reproduced from Ref. [103] with permission. Copyright (2016) The Royal Society of Chemistry.

(Figure 4c). The carefully selected 1,2,4,5-benzene tetracarboxylic acid (BTAC) precursor endows the obtained carbon (BTCADC) with a porous network structure (Figure 4d). After further activation treatment, the curved sheet-like and highly porous features carbon (A-BTCADC) was obtained (Figure 4e). Lastly, the A-BTAC derived carbon cathode was matched with LTO for fabricating a LIC, which could achieve an energy density of 63 Wh/kg with a good cyclability (6000 cycles). Hence, the functionalized or controlled porosity of graphene might provide the opportunity to replace the commercial AC in LIC cathode materials ultimately.

From another perspective, the construction of 2D graphene into 3D porous graphene opens a new avenue for rapid charge storage. Wang et al.[102] fabricated a LIC with a 3D porous graphene hydrogel (via a simple hydrothermal process) as the cathode and TiO_2 nanobelt arrays (NBAs) as the anode. The free-standing porous graphene hydrogel (Figure 4f) was directly used as the electrode, which showed an excellent capacity of 52 mAh/g. The LIC device (Graphene hydrogels//TiO_2 NBAs) yielded maximum energy of 82 Wh/kg and a high power density of 19 kW/kg (Figure 4g). Similarly, Zhang et al.[103] synthesized 3D porous graphene-based materials (3Dgraphene) by hydrothermal and KOH activated process (Figure 4h). The as-prepared electrode provided a high electrochemical performance, which is derived from the increased specific surface area and ionic/electronic conductivity of 3DGraphene. Based on this, a LIC device was integrated with a high capacity Fe_3O_4/graphene nanocomposite (Fe_3O_4/G) as anode and a 3DGraphene as a cathode, which achieved energy densities of 147–86 Wh/kg and power densities from 150 to 2587 W/kg. Later, Ye et al.[45] reported a rich macro/mesoporosity of 3D porous graphene macro-foam (PGM) as a high-performance LIC electrode. The improved performance of graphene is due to the construction of 3D porous frameworks. The unique 3D structure could balance the space, provide more opportunities to contact electrolyte ions, and shorten the ion diffusion path. Therefore, the assembled PGM//LTO/C LIC device demonstrated an energy density of up to 72 Wh/kg and a power density of 8.3 kW/kg.

In a word, graphene materials exhibit very high capacity and energy as cathode materials for LICs, but at the same time, some problems still exist.[104–105] One is that a meticulous and complicated synthesis route is usually required to obtain graphene with appropriate structure and surface composition. Another is the technology and cost issues of large-scale production of high-quality graphene for commercial development. Some follow-up fundamental research and further practical application about graphene still need to be carried out.

2.4. Other Porous Carbon Materials

In addition to the AC, TC, and graphene described above, there are also many other carbon materials used in LICs cathodes, such as one-dimensional (1D) carbon nanotubes (CNTs), porous carbon fibers, 2D/3D porous carbon, and carbide-derived carbons (CDCs). Zhao et al.[106] integrated a LIC device by a multi-walled CNT (MWCNT) film (grown by CVD) as a cathode and a α–Fe_2O_3/MWCNT film as an anode. The flexible LIC achieved an energy density of 50 Wh/kg and a power density of 4 kW/kg. Later, Shi et al.[107] successfully prepared an activated carbon nanofiber (a-PANF) by a bottom-up electrospinning technique (Figure 5a). The highly graphitized and hierarchical porous structure of a-PANF materials could deliver a discharge capacity of 80 mAh/g at the current density of 0.1 A/g (Figure 5b and c). Furthermore, a high-performance LIC was assembled by using a-PANF as the cathode and Fe_3O_4 as the anode, which exhibited energy densities of 123.6–103.7 Wh/kg, and power densities increased from 93.8 to 4687.5 W/kg. The unique spatial structure and high conductivity of 1D carbon materials as LIC cathode enhance the high power performance of the device. However, the complicated purification process, relatively low capacity, and high preparation cost impede their wide commercial application. Some further researches are still demanded to deal with the above issues.

In parallel to 1D carbon materials, the utilization of 2D/3D porous carbon materials as LIC cathode has been widely reported. For example, 2D B/N codoped carbon nanosheets (BNC, Figure 5d) were used as cathodes to fabricate a high-performance LIC by Hao et al.[108] The unique structure of 2D materials and heteroatom doping can boost active storage sites and conductivity. Thus, the energy and power density of the devices could achieve 149.5 Wh/kg and 35 kW/kg, respectively (Figure 5e). The life span of the LIC was pretty good with 90.5% capacity retention after 10000 cycles (Figure 5f). Besides, Yang et al.[109] synthesized a 3D porous N-doped carbon (HNC) material with multi-type open pores structure, which could provide a large external surface area. The LIC device based on a high capacity (62 mAh/g) HNC cathode and MnO-graphene composite (MnO@GNS) anode (Figure 5g), revealed energy densities of 127–83.25 Wh/kg and power densities range of 125–25000 W/kg, but only 81% capacity remained after 2000 cycles. Similarly, Lee et al.[110] designed a LIC by using a 3D amorphous carbon (3DaC) as a cathode and a high capacity $MnFe_2O_4$/carbon (MFC) as an anode. The 3DaC materials could alleviate the decomposition of electrolytes in high voltage, which improved the stability of the LIC cathode. The energy density of the assembled LIC could up to 157 Wh/kg with enhanced capacity retention (86.5% after 6000 cycles). Besides, the porous CDC, whose pore size distribution and particle size could be finely controlled, also has been extensively applied in model EES devices. Rauhala et al.[111] constructed a LIC based on a CDC cathode coupled with a PLG anode, which could deliver the maximum energy density of about 90 Wh/kg. Overall, it is worth noting that some of the 2D/3D carbon materials have been gradually applied to practical production due to their preparation process is simple, low-cost, controlled porosity, and high properties.

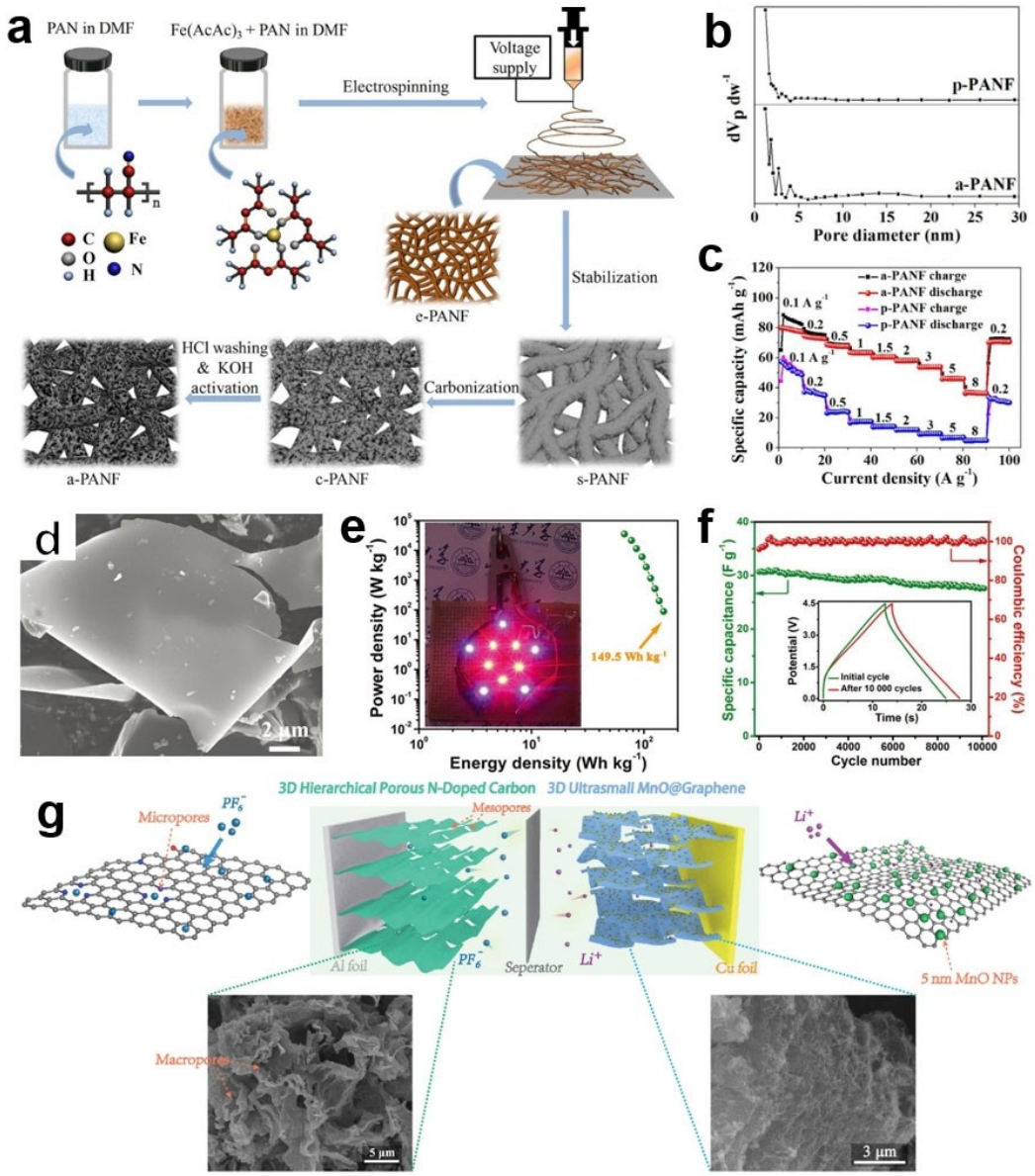

Figure 5. a) Detailed schematic diagram of a-PANF synthesis. b) Pore-size distributions and c) rate-performance of a-PANF and p-PANF materials. Reproduced from Ref. [107] with permission. Copyright (2018) Wiley-VCH. d) SEM image of BCN sheets. e) Ragone plot and f) cycling performance of SnS_2/RGO//BCN LICs. Reproduced from Ref. [108] with permission. Copyright (2019) Wiley-VCH. g) Schematic diagram of the MnO@GNS//HNC LIC device, together for the SEM images of both cathode and anode materials. Reproduced from Ref. [109] with permission. Copyright (2015) Wiley-VCH.

2.5. Composite Carbon Materials

As mentioned above, the capacity of the cathode material seriously affects the energy density of the LIC. Therefore, the development and design of carbon material cathodes with high capacity and high rate performance is particularly critical. However, most carbon materials have more or fewer limitations when they are used as electrode materials alone, such as the relatively low conductivity of porous materials, low capacity of CNT, and easy agglomeration of 2D graphene sheets.[112] Based on this, it is easy to come up with an idea to composite different carbon materials for acquiring better properties electrode materials. Moreover, composite carbon materials can effectively combine their respective advantages and have been applied as cathode materials for LIC devices in many reports.

In a typical example, Salvatierra et al.[113] successfully prepared a graphene-CNT (GCNT) composite material by a water-assisted hot filament CVD method. High-density CNTs grew directly on the graphene surface to form a seamless contact structure (Figure 6a), which could improve the conductivity of the composite materials. The LIC based on a GCNT cathode and a pre-lithiated GCNT anode demonstrated a high energy density of 121 Wh/kg and a high power density of 20.5 kW/kg. The capacity retention of the obtained LIC could maintain about 89% after over 10000 cycles (Figure 6b). Subsequently, a 3D single-wall CNT/graphene composite net-

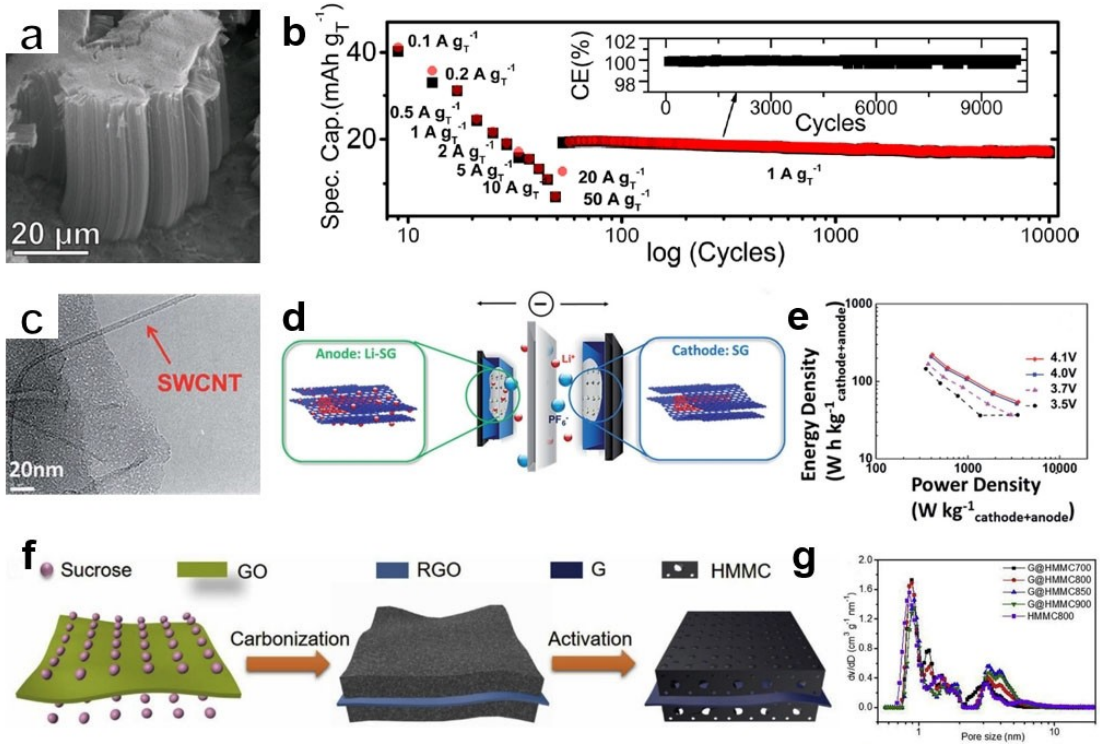

Figure 6. a) SEM image of the growth of CNT on the graphene surface. b) Rate-performance and long cycling stability of GCNT-based LIC. Reproduced from Ref. [113] with permission. Copyright (2017) American Chemical Society. c) A TEM image of SG. d) Schematic diagram of the SG//Li–SG LIC device. e) Ragone plots of the SG//Li–SG LIC worked various voltage ranges. Reproduced from Ref. [114] with permission. Copyright (2017) The Royal Society of Chemistry. f) Scheme of the preparation process for G@HMMC materials. g) Pore-size distribution of HMMC and G@HMMC materials. Reproduced from Ref. [116] with permission. Copyright (2018) Elsevier.

work (SG) was provided by Sun et al.[114] The CNTs were well embedded and distributed in graphene sheets (Figure 6c), which not only enhanced the electric conductivity and porosity of the SG materials but also prevented the restacking of graphene. A LIC was integrated with the SG cathode and the pre-lithiated SG anode (Li-SG) (Figure 6d), which could reach the maximum energy density of 222 Wh/kg (Figure 6e) and capacity retention of about 58% after 5000 cycles in the voltage range of 0.01–4.1 V. In addition to CNTs, some other 1D carbon materials have been also applied in composite materials. Liu et al.[115] reported a polyaniline nanotube derived 1D carbon composited with 3D graphene sheets (3D PANI/GNSs) as a cathode, matching with a 3D MoO_3/GNSs foam as an anode to assemble a LIC. The transmission rate of electrons and ions in composite materials was enhanced by constructing a continuous three-dimensional conductive network. The as-prepared LIC device showed energy densities of 128.3–44.1 Wh/kg, power densities from 182.2 to 13500 W/kg, and capacity remained about 90% after 3000 cycles. Furthermore, novel graphene and hierarchical meso-/micro-porous carbon composite material (G@HMMC) were designed by Li et al (Figure 6f).[116] The appropriate amount of oxygen-containing functional groups, hierarchical porous structure (Figure 6g), and abundant sp^2 carbon improve the conductivity and capacity of the composite material. A LIC based on the G@HMMC cathode combined with the PLG anode could acquire energy densities range of 233.3–143.8 Wh/kg, power densities of 450.4–15700 W/kg as well as a stable cycling life (90.6% capacity retained for 3000 cycles). In conclusion, complementary to the inherent properties of pure carbon materials, hybridization can adequately improve the electrochemical properties of the composite carbon materials. The high conductivity and high capacity of graphene composite with 1D CNT or hierarchical carbon materials, which can not only form an effective interconnected conductive network with a high surface area but also promote the ions transmission and achieve a high reversible capacity. Due to these rational properties, the composite carbon material prepared in a facile and practicable way is a critical study direction in the application of high electrochemical performance LIC cathode.

3. Carbonaceous Anode Materials in LICs

In addition to being used as capacitor-type materials, carbonaceous materials can also be utilized as battery-type materials in LIC anodes. To realize the high properties of LIC device with a high energy density, enhanced power performance, and excellent cycle life, the anode materials of LICs need careful selection and reasonable structural design. In recent years, although thousands of battery-type materials have been reported to be applied in LIC anode electrodes, only a few of them can be available for commercial applications.[59] Among them, carbonaceous materials and LTO are two typical anode

electrode materials that are widely used in LICs. Despite the superior structural stability, the high voltage platform (~1.5 V) of LTO versus Li/Li$^+$ limits the energy output of LIC devices.[37] However, carbonaceous materials with appropriate capacity, low voltage operating platforms, and high electronic conductivity meet the requirements of LIC devices with high-performance requirements quite well. At present, battery-type carbonaceous materials generally include graphite, hard carbon (HC), soft carbon (SC), and graphene, which are extensively applied in LIC anodes.

However, the carbonaceous materials anode faces a very serious problem, that is, due to the formation of solid electrolyte interphase (SEI) film on the surface of the carbonaceous material and some parasitic reaction during the first charge-discharge process, a large number of lithium ions in the electrolyte are consumed.[117] The irreversible loss of lithium ions imperils the energy and long-cycle lifespan of LIC devices. To tackle this issue, pre-lithiation technology is an effective method to enhance the performance of LICs. The pre-lithiation process is usually carried out before the cycle test of LIC devices, which can not only alleviate the loss of lithium ions and improve the cycle stability but also increase the operating voltage range between the cathode and anode electrodes.[118–119] Thus, the pre-lithiation treatment of carbonaceous materials anode is particularly important for increasing the energy output of the entire LIC device.

3.1. Graphite/Graphitized Materials

As an allotrope of carbon, graphite has the characteristics of high reversible capacity and low lithium intercalation potential platform (below 0.2 V vs Li/Li$^+$).[26] Graphite is self-assembled from graphene nanosheets with a honeycomb crystal lattice structure through van der Waals forces, and the layer distance is about 0.335 nm.[120] The energy storage in graphite occurs in the graphene layer with a reversible insertion/extraction process of Li$^+$ ions, and the corresponding capacity-potential curve is shown in Figure 7a. The interaction process of lithium-ion into graphite can be described by the formula as [Eq. (1)]:[121–122]

$$xLi^+ + C_6 + xe^- \leftrightarrow Li_xC_6 \quad (1)$$

As shown in Figure 7a, the multiple-stage process of lithium-ion inserts into graphite could interpret by Daumas-Herold model.[123–124] The theoretical capacity of graphite can be reached to 372 mAh/g with about 10% volume variation, and

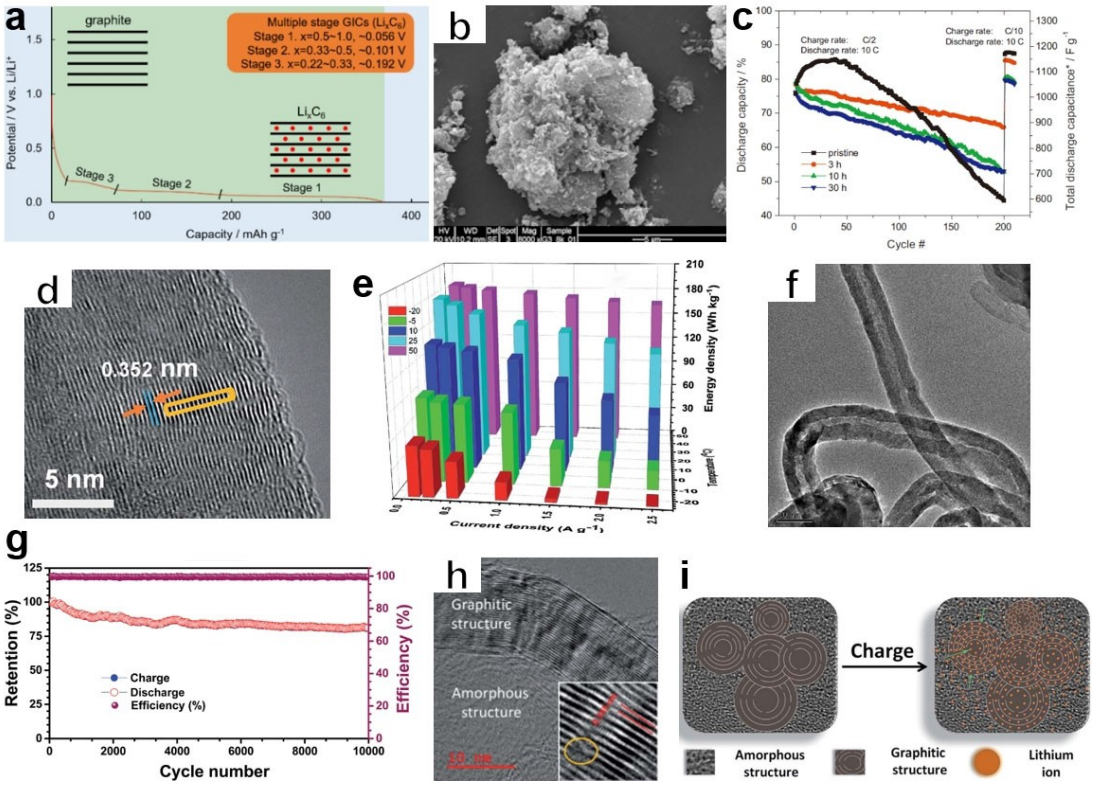

Figure 7. a) Capacity-potential curve and schematic diagram of lithium-ion inserts into graphite. Reproduced from Ref. [17] with permission. Copyright (2020) Wiley-VCH. b) SEM image of 3 h-milled graphite materials. c) Cycling performance of the pristine and ball-milled graphite at various charge/discharge C-rates. Reproduced from Ref. [125] with permission. Copyright (2011) Elsevier. d) HR-TEM image of RG and e) 3D plots of the DC-LIC indicating the relation of energy density values with temperature for different current densities. Reproduced from Ref. [126] with permission. Copyright (2020) The Royal Society of Chemistry. f) TEM image of VO–CF materials. Reproduced from Ref. [127] with permission. Copyright (2018) Elsevier. g) Cycling and CE profiles of the CO–CS-based LIC at 1.5 A/g current density. Reproduced from Ref. [128] with permission. Copyright (2018) The Royal Society of Chemistry. h) TEM images and i) the charge storage mechanism of GC1100. Reproduced from Ref. [129] with permission. Copyright (2017) The Royal Society of Chemistry.

the capacity obtained below 0.3 V is dominant. After the pre-lithiation process, the potential of graphite anode usually can be maintained at about 0.1 V, which greatly increases the voltage output of LIC devices. Thus, the pre-lithiated graphite-based LICs can acquire a high energy density, which has been confirmed by a series of literature reports.

Khomonko et al.[130] fabricated a high-performance LIC based on commercial graphite anode and AC cathode in an organic electrolyte. By balancing the mass ratio of the electrode and operating voltage range of the LIC device, a high energy density of 103.8 Wh/kg could be achieved as well as a prolonged lifespan. Besides, Sivakkumar's group investigated the performance of ball-milled graphite as anode electrode in LIC compared with pristine commercial graphite.[125] After the ball milling process, the degree of crystallinity of graphite reduced, and the amorphous state increased accordingly. This resulted in two energy storage mechanisms for ball-milled graphite: lithium-ion insertion-type and adsorption-type, and the later mechanism dominated the capacity. The LIC based on 3 h-milled graphite exhibited a high rate performance and long cycle-life (Figure 7b and c). Recently, an efficient method for treating graphite recovered from waste LIBs as anode material for LICs was proposed by Divya et al.[126] After essential treatment, the obtained recovered graphite (RG) had a larger interlayer spacing (0.352 nm, Figure 7d) than that of pristine graphite (0.339 nm), which is derived from the continuous Li^+ ion insertion/extraction process in graphite anode before recycling. Based on the RG as anode and AC as a cathode, the fabricated DC-LIC device achieved an energy density of 185.54 Wh/kg and possessed a wide temperature operating range (Figure 7e). However, the poor-rate capability of graphite caused by the sluggish kinetics of the Li^+ ion insert process limits the power performance of LIC. Aiming to resolve it, Cai et al.[131] prepared a multi-walled CTN/graphite composite material (MWCNT/graphite) as anode for fabricating LIC. With an appropriate content of highly conductivity MWCNT, the MWCNT/graphite-based LIC revealed the maximum energy density of 96 Wh/kg, and the power density could be increased to 10.1 kW/kg. The capacity retention was about to 86% after 3000 cycles.

To further improve the properties of graphite, it can also be realized by adjusting the structure and morphology of graphite, such as ultra-layered graphite,[132–133] and highly graphitized carbon materials.[134] Graphitic carbon (GC) has both a graphite structure and an amorphous structure, which is generally obtained by graphitizing a carbon-rich precursor at a moderate temperature ($<1200\,^{\circ}C$) with the assistance of a metal ion catalyst.[129,135] For example, Jayaraman et al.[127] proposed a hollow 1D graphitic nanofiber (VO-CF, Figure 7f), which was prepared by a modified CVD method with the carbon source of vegetable oil. The unique 1D structure and porosity enhance the conductivity and ion transmission capacity of VO-CF materials. Hence, the integrated LIC with AC as the cathode and pre-lithiated VO-CF as the anode delivered a high energy density of 112 Wh/kg and capacity retention of 67% after 10000 cycles. Furthermore, the same group[128] also reported a GCs with a spherical morphology (CO-CS) by a similar method. The pre-lithiated CO-CS-based LIC exhibited the maximum energy density of 108 Wh/kg and good cycle stability with 81% capacity maintained after 10000 cycles (Figure 7g). In addition, Yang et al.[129] synthesized GC materials via pre-carbonization and catalytic graphitization treatment using sisal fibers as the raw materials. The high plateau capacity and high rate capability could be acquired for the optimum GC1100 prepared at 1100 °C, which is derived from the coexistence of graphitic and amorphous structure (Figure 7h and i). The LIC assembled by pre-lithiated GC1100 anode match with sisal fiber activated carbon cathode (SFAC-2), revealed energy densities of 104–32 Wh/kg, power densities from 143 to 6628 W/kg, and retention of 96.5% at 1 A/g for 3000 cycles.

In conclusion, although graphite or GC has made good progress as an anode material for LIC in recent years, its rate capability and long cycling stability (low potential easily induces lithium dendrites formation, which might eventually destroy the cell) still need to be improved. Several strategies like control the structure and dimension of graphite, adjust the mass loading, thickness, and porosity of the electrode are feasible to enhance the performance of the graphite electrode.

3.2. Hard Carbon

HC, as a non-graphitizable amorphous carbonaceous material, is usually obtained by pyrolyzing polymers at high temperatures ($<1500\,^{\circ}C$), and it is difficult to graphitize even at high temperatures above 2500 °C. HC can be regarded as a type of small disorderly aggregated graphite particles, which is caused by the abundance of nanovoids present in the material.[136] On account of this, the volume variation of HC is smaller than graphite and provides a higher specific capacity.[137] The storage mechanism and capacity-potential curve of HC are illustrated in Figure 8a. Different from graphite, the potential curve of HC has an obvious slope in stage II, and the energy storage mechanism is also distinguishing. From the stage I to stage III, lithium ions have experienced adsorb on the surface of hard carbon particles at first (red dots), then adsorb between graphene nanosheets (blue dots), and finally under-potential deposition (UPD) of metal Li in the nanovoids (orange dots).[17] Due to the fast Li^+ ion adsorption/desorption processes, the rate capability of HC is superior to graphite. However, the abundant edge active sites exist in HC material will affect the formation of a stable SEI film, and the voltage hysteresis phenomenon causes a low coulombic efficiency (CE) at the initial cycle.[26] In particular, the pre-lithiation treatment for HC has overcome this issue effectively, and the LIC based the pre-lithiated HC anode demonstrate attractive performance in recent years.

In the early stage, Kim et al.[138] investigated the electrochemical performance of various kinds of carbon material (graphite and HC) as anode for LIC devices. Benefiting from the disordered microstructure composed of the cross-linked graphene layer, the process of inserting and extracting lithium ions in the hard carbon material is promoted, thereby enhanced the rate performance of the hard carbon (Figure 8b).

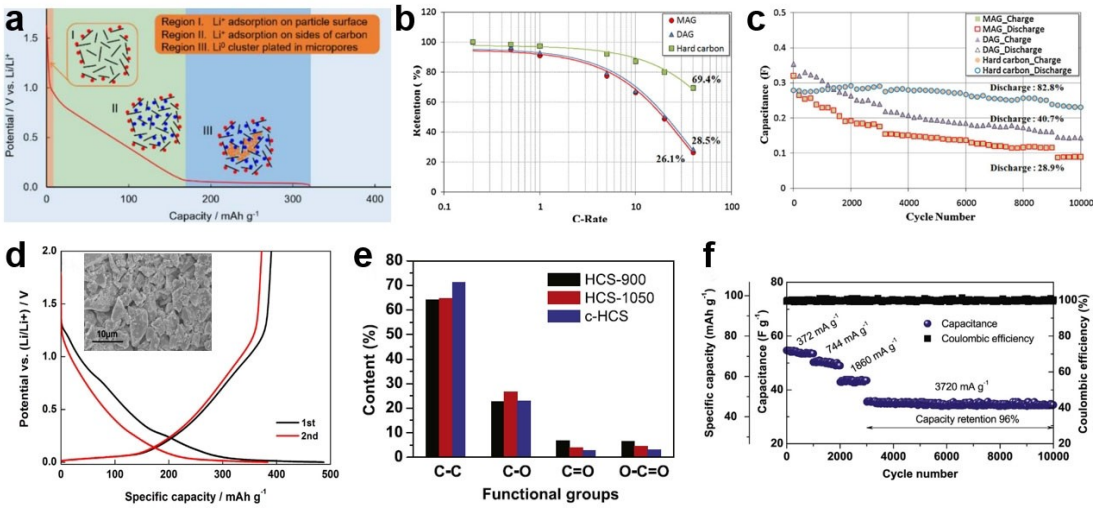

Figure 8. a) Capacity-potential curve and schematic diagram of lithium-ion storage into HC. Reproduced from Ref. [17] with permission. Copyright (2020) Wiley-VCH. b) Rate capability and c) Cycling performance of the LIC devices utilizing various carbon anode materials. Reproduced from Ref. [138] with permission. Copyright (2011) Elsevier. d) Galvanostatic charge-discharge curves of IH at 0.05 C-rate and the insertion is the SEM image. Reproduced from Ref. [139] with permission. Copyright (2015) Elsevier. e) Percentage of various oxygen-containing groups in the as-synthesized o-HCS materials. f) The rate and cycling performance of AC//o-HCS LIC. Reproduced from Ref. [140] with permission. Copyright (2017) Elsevier.

Thus, the HC-based LIC revealed a better rate capability and cycle stability (~83% capacity maintained after 10000 cycles) than graphite-based devices, which demonstrated the HC was suitable as LIC anode material for commercial application (Figure 8c). Furthermore, Zhang et al.[139] researched the performance influence of various morphologies HC as anode materials for LIC. Compared to spherical HC, the charge-discharge curve of irregular HC (IH) had an obvious Li^+ ion intercalation platform at a low potential, which is more beneficial to fully utilize the capacity of AC cathode (Figure 8d). Therefore, the LIC based on pre-lithiated IH anode at the voltage range of 2–4 V could deliver an energy and power density of 87.5 Wh/kg and 7.6 kW/kg, respectively. A superior cycling performance could be achieved with 96% retention after 5000 cycles. To enhance the performance of HC as anode for the LIC device, some researchers have focused on the modification of HC. For example, a sphere-type HC with surface oxygen-containing functional groups (o-HCS) was prepared via a facile oxidative approach by Fu et al.[140] The appropriate doping of oxygen (Figure 8e) not only increased the pseudocapacitance storage but also enhanced the lithium-ion diffusion, thus the obtained o-HCS material had an improved high-rate and cycle performance. Lastly, the LIC by using pre-lithiated o-HCS anode coupled with AC cathode could still exhibit a capacitance of 34.8 F/g even at a high current density of 3720 mA/g, and long cycle stability with only 4% capacity degradation after 7000 cycles (Figure 8f). Besides, some researchers are also dedicated to investigating various lithium sources for the pre-lithiation treatment of HC, such as stabilized Li metal powder (SLMP)[141] and thin lithium stripes,[142] which is capable to solve the shortcomings of hard carbon and simplify the process of preparing LICs.

From the above results, we can conclude that different microscopic morphologies and structures have a crucial influence on the capacity and rate performance of HC. The electrochemical performance of HC can be improved by introducing heteroatoms (O, N), adjusting the porosity or micro-morphology of the materials.

3.3. Soft Carbon

Another type of amorphous carbon, SC, is a carbon material that can be graphitized above 2500 °C. Similar to the production of HC, SC is usually obtained by pyrolyzing biomass carbon materials (like cokes and chars) at 800 ~ 1500 °C.[17] However, compared with HC, SC consists of thin graphene nanosheets that have fewer nanovoids defects and relatively a small amount of crystallization. Therefore, SC has high electronic conductivity, and its interlayer space and graphitization degree can be further adjusted by the heat-treat process.[121,143] The charging mechanism and capacity-potential curve of SC are illustrated in Figure 9a. The potential curve of SC is similar to HC, which has a slope in stage II. However, just as the situation of HC, the initial CE of SC is also lower than graphite, thus the pre-lithiation process of SC is essential for the LIC devices. To solve this issue, several approaches have been proposed to obtained pre-lithiated SC electrodes, such as electrochemical method, external short circuit, or direct contact with the auxiliary of metal lithium including sacrificial metallic lithium electrode (SMLE) or SLMP.[119,144] Benefited from this, many reports about SCs for example graphitizable petroleum coke (PeC), have been applied as anodes for high-performance LICs.

Interestingly, Schroeder et al.[148] investigated the influence of an SC (PeC) as anode material for the life-span of LIC. In an appropriate organic electrolyte, an excellent long cycle lifespan (50000 cycles) could be achieved for the PeC-based LIC device.

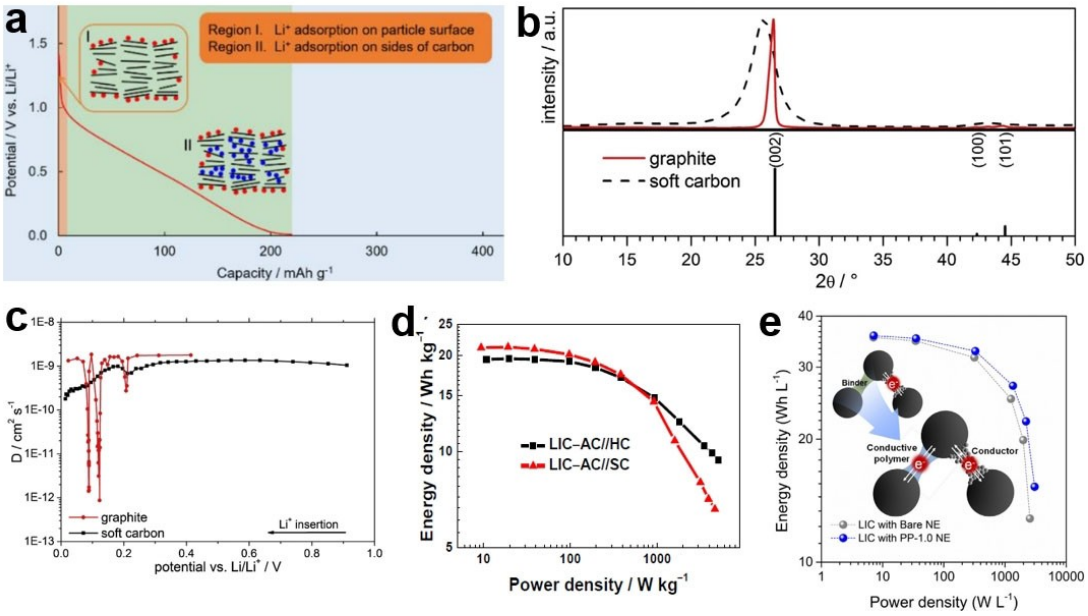

Figure 9. a) Capacity-potential curve and schematic diagram of lithium-ion storage into SC. Reproduced from Ref. [17] with permission. Copyright (2020) Wiley-VCH. b) Power X-ray diffraction (XRD) and c) Galvanostatic Intermittent Titration Technique (GITT) measurements of soft carbon (PeC) and graphite. Reproduced from Ref. [145] with permission. Copyright (2014) Elsevier. d) Ragone plots for the AC//SC and AC//HC LIC devices. Reproduced from Ref. [146] with permission. Copyright (2019) Journal of Electrochemistry. e) Ragone plots for both bare SC and PP-SC based LIC devices. Reproduced from Ref. [147] with permission. Copyright (2015) Elsevier.

And at a high current density of 4.5 A/g, the device also exhibited a power and energy density of 9 kW/kg and 48 Wh/kg, respectively. Furthermore, the same group[145] also compared the structure and electrochemical properties of various carbon materials (graphite and PeC) as an anode electrode for LIC. Different from graphite, PeC had low crystallinity and large interlayer spacing, which are beneficial for the charge transfer and Li-ion diffusion (Figure 9b and c). Therefore, the energy density of PeC based LIC could reach 80.6 and 37.2 Wh/kg at 5 C- and 15 C-rates, respectively. This result was about 20% (at 5 C) and 30% (at 15 C) higher than graphite-based LIC, demonstrated the application of SC as an anode electrode in LICs is very promising. On the other hand, the pre-lithiation degrees of SC also affected the whole performance of LIC devices. Li et al.[146] made a comparative investigation of pre-lithiated HC and SC as anode for LICs devices. By controlling the pre-lithiation capacity of the anode, the prepared AC//SC LIC delivered the highest energy density of 21.2 Wh/kg, while the AC//HC possessed the highest power density of 5.1 kW/kg (based on the whole device, Figure 9d). Besides, incorporating highly conductive material or surface modification is also a possible avenue to improve the property of SC for the high-performance LIC device. In view of this, Lim et al.[147] successfully combined poly(3,4-ethylene dioxythiophene)-polystyrene sulfonate (PEDOT-PSS) into SC as an anode material (PP-SC) for LICs. The highly conductive PEDOT-PSS polymer not only reduced the charge transfer resistance but also enhanced the lithium-ion insertion kinetics in SC material. The as-prepared LIC based PP-SC anode revealed improved energy and power performance with about 85% capacity maintained after 5000 cycle tests (Figure 9e). From this, we can conclude that after solving the problems like initial CE and conductivity, the application of SC material as an anode electrode for high properties and long cycle stability LIC devices will be more favorable.

3.4. Graphene

Interestingly, besides as a cathode material, graphene has also been recognized as a very promising anode material for LIC devices. Unlike graphite, single-layer perfect graphene can storage Li^+ ions on both sides with a stoichiometry form of Li_2C_6, which affords a specific capacity of 744 mAh/g in theory – that double of graphite (372 mAh/g).[121] In terms of mechanism, lithium ions can not only be adsorbed on both internal surfaces of single-layer graphene, but also in nanovoids that caused by the randomly arranged graphene layer (conform to the 'house of card' model).[121,149] This behavior is similar to some amorphous carbonaceous materials but differs from the staging ion intercalation behavior of graphite.[123] Based on the unique mechanism, the preparation way of the graphene electrode largely determines the amount of lithium stored in the graphene anode.[150]

On the other hand, the irreversible capacity of graphene materials (such as reduced graphene oxide, denoted as rGO) in the initial cycles is usually very high, which is resulted from the high specific surface area of graphene promotes the formation of SEI.[150] Besides, the existence of voids, edges, and functional groups in graphene induces a voltage hysteresis phenomenon during the charging/discharging process.[151] Furthermore, the tendency of re-stacking for graphene nanosheet strongly

impedes the full utilization of Li^+ storage capacity among the subsequent cycle test.[93] Thus, the problem of rapid capacity decay and poor cycle performance usually emerge when graphene is utilized as anode materials. In this respect, the pre-lithiation technique is an effective strategy to improve the initial CE of the electrode and supply lithium-ion to the electrolyte. In addition, from the point of materials, it is also available to synthesize high-quality graphene, modify the surface of the graphene, or design graphene-based composites to prevent graphene from re-stacking and improve the performance of the anode electrode.[59,152]

As mentioned above, the preparation ways of materials and electrodes are essential to the properties of graphene anode. In the early stage, Ren et al.[153] prepared pre-lithiated graphene nanosheets as anode and AC as cathode for assembling a LIC. Compared with graphite, the cross-linked graphene nanosheets (via chemical exfoliation) with a hierarchical pore structure provided higher capacity, better cycle performance, and enhanced lithium-ion diffusion rate. Meanwhile, the pre-lithiated graphene nanosheets based LIC showed a maximum power density of 222.2 W/kg with a corresponding energy density of 61.7 Wh/kg (Figure 10a). To improve the energy density of LIC, Ahn et al.[154] provided a facile method to fabricate a 3D highly oriented rGO sponge (HOG) as a high-performance anode for LIC devices. The unique 3D porous structure of HOG as the anode provided high capacity and long cycling stability. Furthermore, the HOG was directly pre-lithiated by an internal short-circuit method to apply as an anode. When coupled with an AC cathode, the AC/HOG–Li LIC demonstrated superior energy densities of 231.7–131.9 Wh/kg, power densities from 57 to 2800 W/kg, and about 84.2% capacity maintained after 1000 cycles (Figure 10b). Besides, the high quality of graphene powder was also proposed by Li et al, through a scalable self-propagating high-temperature synthesis (SHS) using the carbon source of CO_2.[155] Based on the high conductivity (~13000 S/m), high specific surface area (~700 m^2/

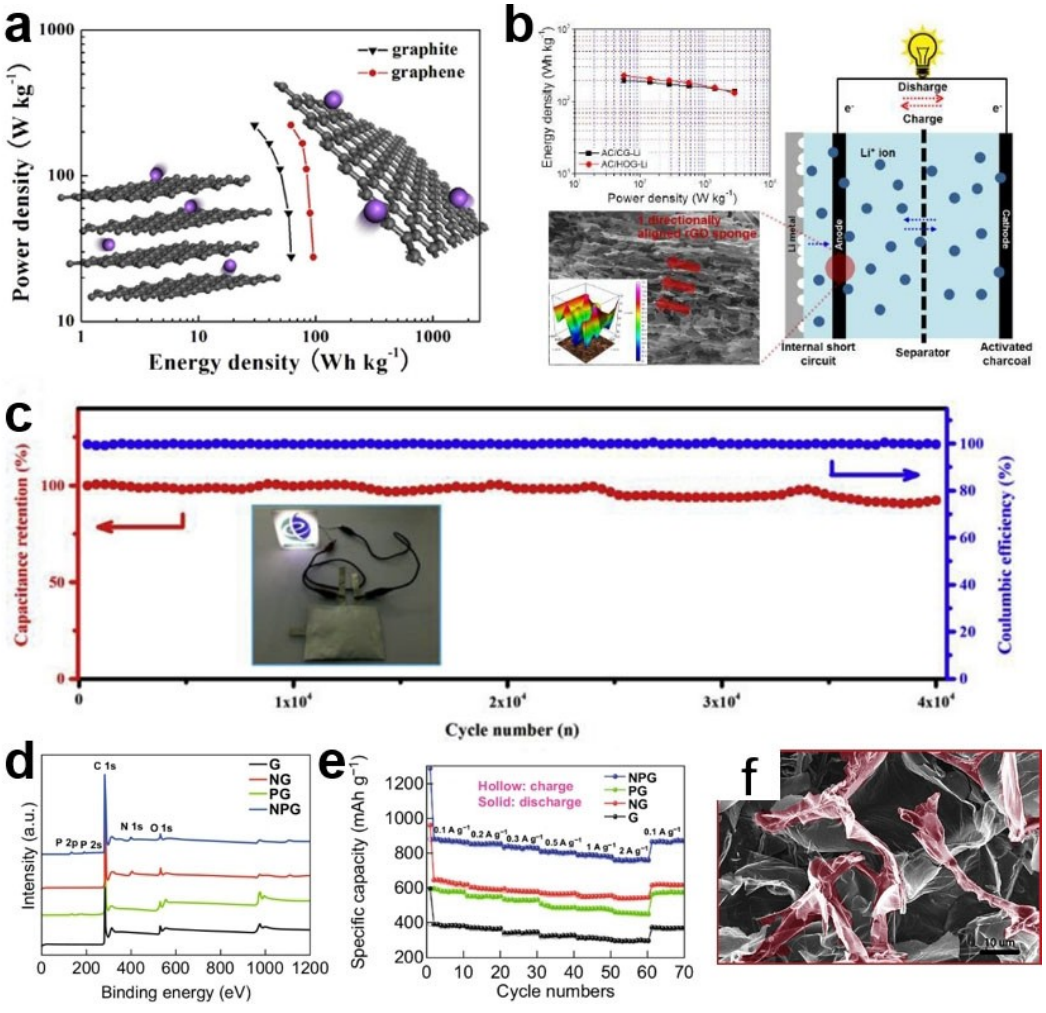

Figure 10. a) Ragone plots for the LICs based on pre-lithiated graphite and graphene anode, respectively. Reproduced from Ref. [153] with permission. Copyright (2014) Elsevier. b) Ragone plots and schematic illustration of the AC/HOG–Li LIC device configuration, the insertion are the SEM and 3D mapping chemical intensity images of HOG. Reproduced from Ref. [154] with permission. Copyright (2016) American Chemical Society. c) Cycling performance of SHSG-based LIC at a current density of 4 A/g. Reproduced from Ref. [155] with permission. Copyright (2018) Elsevier. d) Full and high-resolution and e) rate capabilities of the NPG compared with various graphene materials. Reproduced from Ref. [156] with permission. Copyright (2019) The Authors .f) SEM image of the cMEGX. Reproduced from Ref. [157] with permission. Copyright (2017) Elsevier.

g), and abundant mesoporous structure of prepared graphene as the anode (SHSG), the assembled LIC achieved energy densities of 146–103 Wh/kg, power densities range of 650–52000 W/kg. A remarkable life-span of the LIC was also provided with about 91% capacitance reserved after 40000 cycles (Figure 10c), much higher than the data previously reported in the LIC devices.

To further improve the performance of graphene anode, heteroatoms doping has been proved to be an effective strategy to adjust the surface electronic structure and enhance the storage capability of Li^+ ions. Luan et al.[156] designed N and P co-doped multilayer graphene (NPG) material by using graphite and $(NH_4)_3PO_4$ powders as sources. Benefited from the N and P doping (Figure 10d), the NPG anode achieved a high reversible capacity, high rate capability as well as good cyclability (Figure 10e). Moreover, the NPG based LIC devices delivered energy densities from 195 to 77 Wh/kg, power densities of 746.2–14983.7 W/kg. Besides, graphene composite with carbon materials is also a feasible solution to enhance the storage kinetics of lithium-ion. For example, a 3D melamine based carbon/rGO composite sponge (cMeG) was synthesized by Tjandra's group.[157] The melamine foam was directly applied as both carbon and N resource, thus a free-standing 3D composite electrode could be obtained by coating GO and then the carbonization process (Figure 10f). The LIC based on cMeG anode delivered an energy density of 40 Wh/kg. Similarly, Kim et al.[158] investigated the electrochemical behavior of graphene nanoplatelet (GNP)-CNT hybrid materials as anode for LIC. The highly conductive CNT was directly grown on the surface of GNP by the CVD approach. Due to the unique combination of 1D and 2D structures, the GNP-CNT-based LIC exhibited an energy density of 116 Wh/kg, a power density of 11 kW/kg, and capacity retained about 72.8% after 5000 cycles. The strong contact of GNP-CNT composite material made it suitable for a high-performance LIC anode. However, even though many investments have demonstrated the graphene as a promising candidate for LIC anode, the meticulous design of the graphene structure and the weight ratio distribution of different components in the composite are still critical problems that must be dealt with to acquire good electrochemical properties and prolong cycle life.

3.5. Other Carbon Materials

In addition to the carbonaceous materials described above, other various kinds of carbon materials have also been exploited and took into account as anode electrodes for LICs in the aspect of energy and cycle stability. Xia et al.[159] synthesized N and B co-doped 3D porous carbon nanofiber (BNC) in a facile way by using the commercial bacterial cellulose as the precursor (Figure 11a). The fabricated LIC based on BNC anode presented energy densities of 220–104 Wh/kg, corresponding power densities from 225 to 22500 W/kg, and a good cycle performance (about 81% retention after 5000 cycles). The enhanced performance of BNC based LIC was attributed to the unique 3D interconnected conductive structure, enlarged interlayer spacing, and improved lithium diffusion kinetics with B and N co-doping. Then, N and O co-doped (derived from the gelatin) porous carbon nanosheets (NOPCNs) was also provided by Liu's group with the assistance of ice/KCl both as templates.[160] The obtained NOPCNs possessed the properties of hierarchical porous structure (Figure 11b and c), high electronic conductivity, and abundant heteroatoms, thus endowing the NOPCNs based LIC with improved rate and cycling performance. The fabricated LIC device could achieve a high energy density of 184 Wh/kg, a power density of 78.1 kW/kg, and an extended cycle life with 70% energy retention after 10000 cycles. Moreover, Dubal et al.[161] reported N-doped carbon nanopipes (N-CNPipes) were utilized as high-performance anode materials for LIC devices. The unique structure of N-CNPipes not only promoted close contact with electrolytes but also facilitated the diffusion rate of Li^+ ions from both the exterior and interior of carbon nanopipes (Figure 11d). Because of this, the N-CNPipes based LIC device yielded high energy densities of 262–78 Wh/kg, high power densities range from 450 to 9000 W/kg, and reasonable good cycle stability (only ~9% capacity loss) for 4000 cycles. Another 3D N-doped hollow carbon microsphere (NHCM) was successfully prepared by Jiang and co-workers for high-performance LIC anode material (Figure 11e).[162] The kinetic analysis of the NHCM material revealed a high lithium ion adsorption and diffusion ability, which was due to the N-doping and defect structure (Figure 11f). The assembled LIC device based on NHCM had a high energy density of 162 Wh/kg, a power density of 10.5 kW/kg as well as a good life-span (about 86.2% capacity retained for 5000 cycles).

In summary, carbon materials with heteroatom-doping are available for high energy LIC anode material, which is derived from the improved electrode-electrolyte contact interface, lithium-ion diffusion kinetic, and provide a more active site.

4. Summary and Outlook

The development of advanced LIC devices with high energy and power outputting desires the utilization of electrode materials that possess fast electronic/ion conductivity as well as favorable structural stability. Numerous novel materials as high-performance LICs electrode have witnessed the booming of development and abundant achievements in recent years, yet carbonaceous materials are still the most popular electrodes for practical applications. This review is devoted to involving the electrochemical performance of carbon-based electrodes in LIC devices, which have been prepared and investigated during the past few years. The crucial electrochemical performances of discussed LICs based on carbon materials as anode or cathode are presented in Table 1. We analyzed the application of carbonaceous materials as anode or cathode in high energy and power LIC devices. From this analysis, some critical conclusions could be drawn concerning materials and, also, the fabrication of devices.

To realizing the high energy and power of LIC devices, the capacity and rate capability of carbonaceous materials (as

doi.org/10.1002/batt.202000264

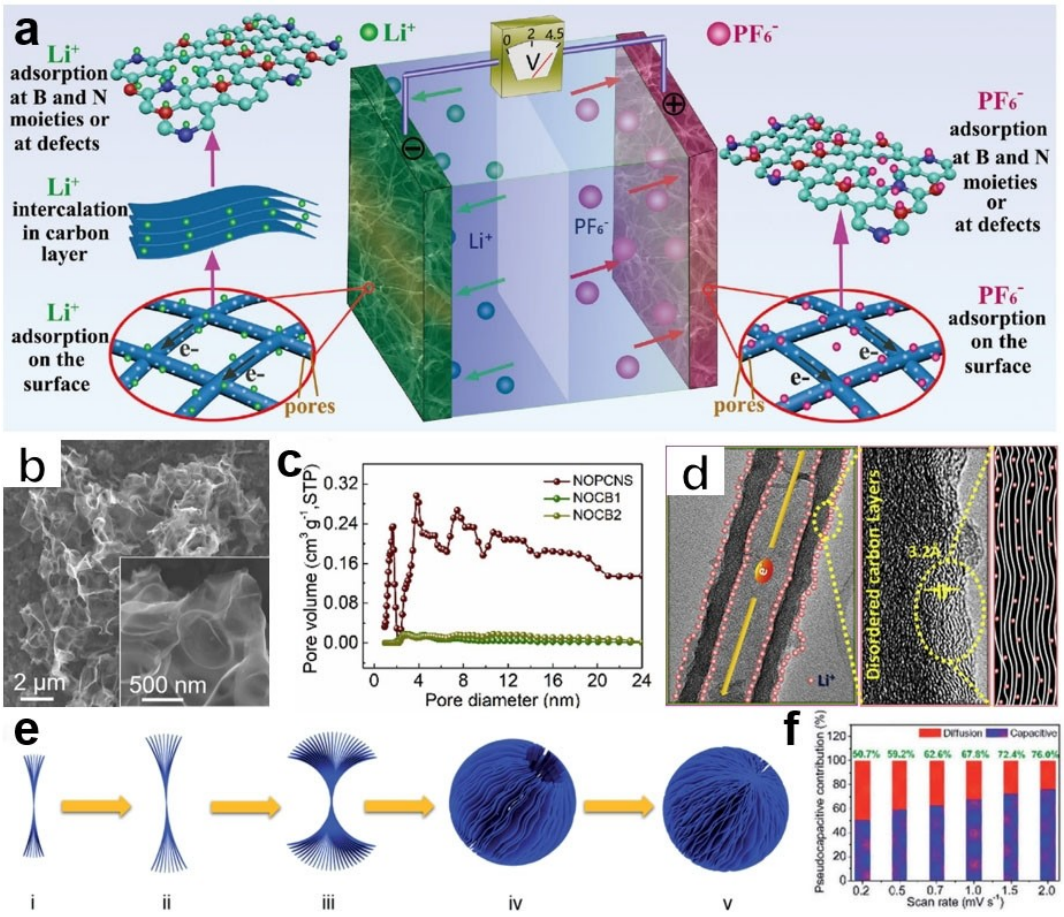

Figure 11. a) Schematic diagram of the energy storage mechanisms for the BNC-based LICs. Reproduced from Ref. [159] with permission. Copyright (2017) Wiley-VCH. b) SEM images and c) pore size distribution of the NOPCNS sample. Reproduced from Ref. [160] with permission. Copyright (2019) Elsevier. d) TEM and HRTEM images accompany a schematic explanation of the charge storage mechanism for the N-NCPipes. Reproduced from Ref. [161] with permission. Copyright (2018) Elsevier. e) Schematic diagram of the fabrication process for the NHCM sample. f) The capacity contribution proportion of the pseudocapacitance and diffusion-controlled charge versus scan rates for the NHCM anode. Reproduced from Ref. [162] with permission. Copyright (2020) The Royal Society of Chemistry.

anode or cathode) should be enhanced. However, to prepare carbon materials with high quality, high capacity, and cycling stability, complexity, and high costs of fabrication processes are usually needed. In further researches, the preparation steps should be simplified and cut production cost via designing facile, high yield, and low energy consumption approaches. In-situ limitation growth, self-propagating high-temperature synthesis, or flash Joule heating process are feasible approaches to realize scalable production of high-quality carbon materials. The selection of suitable and eco-friendly raw materials also needs consideration.

Another issue to consider is how to close the kinetics and capacity gap between battery-type anode materials and capacitor-type cathode materials. The power output of the LICs devices is limited by the inherent sluggish Li^+ insertion behavior of the bulk anode material. Strategies such as nano-engineering, heteroatomic doping can introduce pseudocapacitive-like kinetics, which could provide fast and reversible electrochemical charge transfer reactions and improve the rate performance of the anode material. The capacity of cathode materials also can be enhanced by exquisite pore structure design or introducing pseudocapacitive reaction mechanisms, which is the key advance in the field of capacitive storage. To realize the LICs devices with promising values of energy and power, introducing high capacity-high voltage materials as cathodes, and the combination of innovative pseudocapacitive materials with high capacity-high rate capabilities anodes will be necessary.

Besides, although the capacity of carbon materials as anodes for LICs is much higher than that of cathodes, it undergoes an inferior initial CE performance. The relatively high surface area of carbon materials and surface defect or functional group (related to various synthetic routes) could be responsible for this. And the energy efficiency of LIC may be hindered when the carbon materials are used as anode directly without any pretreatment. To tackle this problem, the pre-lithiation protocol of anode is essential for LIC devices with desired performances. Yet many types of research have reported the development of pre-lithiation methods in the field of LIC, including sacrificial salts, chemical lithiation, and anode additive lithiation, the large-scale commercialization of these technologies is still limited. Hence, seeking a safe, highly

doi.org/10.1002/batt.202000264

Table 1. Summary of electrochemical performances of carbon-based LICs.

Cathode materials	Anode materials	Voltage window [V]	Maximum energy density [Wh/kg]	Maximum power density [W/kg]	Cyclic number [*n*]	Capacity retention [%]	Ref.
ZHTP	LTO	1–3	69	/	2000	85	[69]
NAC	Si/C	2–4.5	230	30127	8000	76.3	[71]
eAC	Si/C	2–4.5	257	29893	15000	79.2	[72]
a-EW-NaCl	Fe_3O_4@C	1–4	124.7	16989	2000	88.3	[82]
HPC	HPC	1.5–4.5	189	14431	10000	91.3	[83]
MSS-x3-6hr-800 C-A	MSS-x6-6hr-800 C-C	2–4	145	17300	5000	84.8	[84]
MOF-DC	LTO	1–3	65	/	10000	82	[85]
$Zn_{90}Co_{10}$-APC	PLG	2–4	108	15000	10000	/	[86]
URGO	PLG	2–4	106	4200	1000	100	[98]
TRGO	LTO	1–3	45	3300	5000	/	[99]
a-MEGO	Graphite	2–4	147.8	/	/	/	[100]
A-BTCADC	LTO	1–3	63	/	6000	97	[101]
Graphene hydrogel	TiO_2 NBA	0–3.8	82	19000	73	600	[102]
3DGraphene	Fe_3O_4/G	1–4	147	2587	1000	70	[103]
PGM	LTO/C	1–3	72	8300	1000	65	[45]
MWCNT	α–Fe_2O_3/MWCNT	0–2.8	50	4000	/	/	[106]
a-PANF	Fe_3O_4	1–4	123.6	4687.5	1000	85.8	[107]
BNC	SnS_2/RGO	0–4.5	149.5	35000	10000	90.5	[108]
HNC	MnO@GNS	1–4	127	25000	2000	81	[109]
3DaC	MFC	0–4	157	20000	6000	86.5	[110]
CDC	PLG	2–4	90	/	/	/	[111]
GCNT	GCNT	1–4.5	121	20500	10000	89	[113]
SG	Li-SG	0.01–4.1	222	/	5000	58	[114]
3D PANI/GNSs	3D MoO_3/GNSs	0–3.8	128.3	13500	3000	95	[115]
G@HMMC	PLG	2–4.5	233.3	15700	3000	90.6	[116]
AC	Graphite	1.5–4.5	103.8	10	10000	85	[130]
AC	RG	1.8–4.3	185.54	/	2000	75	[126]
AC	MWCNT/graphite	2–4	96	10100	3000	86	[131]
AC	pre-lithiated VO-CF	2–4.3	112	/	10000	67	[127]
AC	pre-lithiated CO-CS	2–4.3	108	/	10000	81	[128]
SFAC-2	GC1100	2–4	104	6628	3000	96.5	[129]
MSP20	HC	1.5–3.9	/	/	10000	83	[138]
AC	pre-lithiated IH	2–4	85.7	7600	5000	96	[139]
AC	o-HCS	2.2–3.8	48.5	3600	7000	96	[140]
AC	PeC	1.5–4	48	9	50000	100	[148]
AC	PeC	0–4	80.6	4800	/	/	[145]
AC	SC	2–4	85.5	/	20000	96.5	[146]
MSP-20	PP-SC	1.5–3.9	/	4000	5000	85	[147]
AC	pre-lithiated graphene	2–4	/	222.2	/	/	[153]
AC	HOG-Li	1.5–4.2	231.7	28000	1000	84.2	[154]
NHCN	SHSG	2–4.5	146	52000	40000	91	[155]
AC	NPG	1–4	195	14983.7	5000	/	[156]
AC	cMeG	2–3.9	/	/	1000	68	[157]
MSP-20	GNP-CNT	2.2–3.8	116	11000	5000	72.8	[158]
BNC	BNC	2–4.5	220	22500	5000	81	[159]
HPC-800	NOPCNS	0–4	184	78100	10000	70	[160]
PRGO	N-CNPipes	0–4	262	9000	4000	91	[161]
NHCM-12	NHCM-A	0–4	162	10500	5000	86.2	[162]

efficient, and low-cost pre-lithiation technique is vital to promote the extensive development of current practical LIC devices.

The accessibility of carbon materials to the electrolyte is also a critical issue to be taken into account. Although surface defects or particle edges may promote ion diffusion to a certain extent, the diffusion of ions into the interior of the carbon material is still quite limited. Nano-engineering is an effective technique to achieve high capacity and provide fast ion diffusion kinetics at once, whereas the prerequisite is to prevent the agglomeration of nanomaterials and ensure the integrity of the structure. This also lies with the structure of prepared carbon materials, likes carbon with nanoribbon, nanoarray, or 3D hierarchical nanoporous structure which could form an intimate contact with the electrolyte and enhance the ion diffusion. The chemical or physical activation process is another avenue to address this problem by reasonably adjusting the pore size distribution of carbon materials.

On the other hand, the realization of LIC devices with high energy and power performance is also correlated with the high operating voltages. To satisfy this characteristic, an innovative and compatible electrolyte with high stability windows (up to 5 V for the carbon-based cathode), high security, and high ion conductivity is the direction that has been pursuing. An appropriate amount of additive in the electrolytes can prominently enhance the performances of the electrode materials, which is derived from the formation of suitable electrolyte-derived thin and stable SEI layers.

At present, the commercial production of carbon-based LICs has made considerable progress, such as JM Energy

Corporation (Japan), Ling Rong New Energy Co., Ltd. (China), etc. However, many challenges still exist that are urgent to be dealt with for the extension of their practical applications, including the density of the material, production costs, the complexity of the preparation process, and so on. Among them, the density of the electrode material is a pivotal factor affecting the volumetric energy density of LICs. Especially in practical applications, the space of energy storage devices is usually restricted. Thus, the exploitation of high-density and high-capacity carbon-based electrode materials to increase the volume performance of LICs is essential. In addition, the development of flexible carbon materials and flexible LICs devices, especially the solid-state flexible LICs, are also critical directions of device construction for the advanced LICs. Based on this, the novel prototypes of high-energy-density LICs devices will be extended to the smart wearable gadgets markets, auxiliary energy equipment, or hybrid and all-electric vehicles and other applications fields in the future.

In summary, the application of carbonaceous materials is undoubtedly a topic of great concern in the domain of electrochemical energy storage. In the future, the investigation in carbon-based materials appropriate to sodium and potassium-based hybrid capacitors will need to intensify, as they also exhibit a prospect in realizing advanced high-performance devices. In parallel, it will be essential to further develop other materials such as MXene, metal oxides, sulfides, etc., which can be used as electrode materials alone or in combination with carbon materials for LICs. Finally, more advanced techniques and theoretical calculations will be demanded to disclose the charge storage mechanism in nanopores of the carbon material and the contact interface with the electrolyte. We expect this review could provide some enlightening and constructive suggestions for researchers who have or will be engaged in this field.

Acknowledgments

This work was financially supported by the National Natural Science Foundation of China (No. 51677182 and 51907193), the Dalian National Laboratory for Clean Energy (DNL) Cooperation Fund, CAS (No. DNL201915 and No. DNL201912), the Key Research Program of Frontier Sciences, CAS (No. ZDBS-LY-JSC047), and the Youth Innovation Promotion Association, CAS (No. 2020000022).

Conflict of Interest

The authors declare no conflict of interest.

Keywords: Li-ion capacitors · carbonaceous materials · energy-power density · energy storage

[1] B. Dunn, H. Kamath, J. M. Tarascon, *Science* **2011**, *334*, 928–935.
[2] Z. Yang, J. Zhang, M. C. Kintner-Meyer, X. Lu, D. Choi, J. P. Lemmon, J. Liu, *Chem. Rev.* **2011**, *111*, 3577–3613.
[3] Y. Xu, K. Wang, J. Han, C. Liu, Y. An, Q. Meng, C. Li, X. Zhang, X. Sun, Y. Zhang, L. Mao, Z. Wei, Y. Ma, *Adv. Mater.* **2020**, *32*, *2005531*.
[4] C. Zhang, H. Zhao, Y. Lei, *Energy Environ. Sci.* **2020**, *3*, 105–120.
[5] S. Song, X. Zhang, C. Li, K. Wang, X. Z. Sun, Q. H. Huo, T. Z. Wei, Y. W. Ma, *J. Energy Storage* **2019**, *24*, 100762.
[6] Z.-Y. Gu, J.-Z. Guo, Z.-H. Sun, X.-X. Zhao, W.-H. Li, X. Yang, H.-J. Liang, C.-D. Zhao, X.-L. Wu, *Sci. Bull.* **2020**, *65*, 702–710.
[7] Z. Liu, J. Wang, B. Lu, *Sci. Bull.* **2020**, *65*, 1242–1251.
[8] M. Li, J. Lu, Z. Chen, K. Amine, *Adv. Mater.* **2018**, *30*, 1800561.
[9] M. R. Palacin, A. de Guibert, *Science* **2016**, *351*, 1253292.
[10] C. Li, X. Zhang, K. Wang, X. Z. Sun, Y. W. Ma, *Chin. Chem. Lett.* **2020**, *31*, 1009–1013.
[11] X. Wu, Y. Bai, Z. Li, J. Liu, K. Zhao, Z. Du, *J. Energy Chem.* **2021**, *56*, 121–126.
[12] J. Yang, D. Xu, R. Hou, J. Lang, Z. Wang, Z. Dong, J. Ma, *Chin. Chem. Lett.* **2020**, *31*, 2239–2244.
[13] P. Simon, Y. Gogotsi, *Nat. Mater.* **2008**, *7*, 845–854.
[14] G. Wang, L. Zhang, J. Zhang, *Chem. Soc. Rev.* **2012**, *41*, 797–828.
[15] X. Zhang, L. Wang, W. J. Liu, C. Li, K. Wang, Y. W. Ma, *ACS Omega* **2020**, *5*, 75–82.
[16] M. Dai, D. Zhao, X. Wu, *Chin. Chem. Lett.* **2020**, *31*, 2177–2188.
[17] S. S. Zhang, *Batteries & Supercaps* **2020**, *3*, 1137–1146; Supercaps **2020**, 3, 1137–1146.
[18] Y. Zhang, Z. Liu, X. Sun, Y. An, X. Zhang, K. Wang, C. Dong, Q. Huo, T. Wei, Y. Ma, *J. Energy Storage* **2019**, *25*, 100902.
[19] J. Zhang, J. Wang, Z. Shi, Z. Xu, *Chin. Chem. Lett.* **2018**, *29*, 620–623.
[20] M. Gyu Jung, G. Sambhaji Gund, Y. Gogotsi, H. Seok Park, *Batteries & Supercaps* **2020**, *3*, 354–360; Supercaps **2020**, 3, 354–360.
[21] G. G. Amatucci, F. Badway, A. Du Pasquier, T. Zheng, *J. Electrochem. Soc.* **2001**, *148*, A930–A939.
[22] N. S. Xu, X. Z. Sun, F. F. Zhao, X. F. Jin, X. Zhang, K. Wang, K. Huang, Y. W. Ma, *Electrochim. Acta* **2017**, *236*, 443–450.
[23] Y. B. An, S. Chen, M. M. Zou, L. B. Geng, X. Z. Sun, X. Zhang, K. Wang, Y. W. Ma, *Rare Met.* **2019**, *38*, 1113–1123.
[24] C. Li, X. Zhang, K. Wang, X. Sun, Y. Ma, *J. Power Sources* **2019**, *414*, 293–301.
[25] C. Li, X. Zhang, K. Wang, X. Sun, Y. Ma, *J. Power Sources* **2018**, *400*, 468–477.
[26] B. Babu, P. Simon, A. Balducci, *Adv. Energy Mater.* **2020**, *10*, 2001128.
[27] B. Li, J. Zheng, H. Zhang, L. Jin, D. Yang, H. Lv, C. Shen, A. Shellikeri, Y. Zheng, R. Gong, J. P. Zheng, C. Zhang, *Adv. Mater.* **2018**, *30*, 1705670.
[28] Y. Firouz, N. Omar, J. M. Timmermans, P. Van den Bossche, J. Van Mierlo, *Energy* **2015**, *83*, 597–613.
[29] H. Jiang, P. S. Lee, C. Li, *Energy Environ. Sci.* **2013**, *6*, 41–53.
[30] X. Z. Sun, Y. B. An, L. B. Geng, X. Zhang, K. Wang, J. Y. Yin, Q. H. Huo, T. Z. Wei, X. H. Zhang, Y. W. Ma, *J. Electroanal. Chem.* **2019**, *850*, 113386.
[31] X. Zhang, J. Miao, P. Zhang, Q. Zhu, M. Jiang, B. Xu, *Chin. Chem. Lett.* **2020**, *31*, 2305–2308.
[32] M. Armand, J.-M. Tarascon, *Nature* **2008**, *451*, 652–657.
[33] X. Z. Sun, X. Zhang, W. J. Liu, K. Wang, C. Li, Z. Li, Y. W. Ma, *Electrochim. Acta* **2017**, *235*, 158–166.
[34] H. Yang, X. Z. Sun, Y. B. An, X. Zhang, T. Z. Wei, Y. W. Ma, *J. Energy Storage* **2019**, *24*, 100810.
[35] K. Naoi, S. Ishimoto, J.-i. Miyamoto, W. Naoi, *Energy Environ. Sci.* **2012**, *5*, 9363–9373.
[36] J. Ding, W. Hu, E. Paek, D. Mitlin, *Chem. Rev.* **2018**, *118*, 6457–6498.
[37] V. Aravindan, J. Gnanaraj, Y. S. Lee, S. Madhavi, *Chem. Rev.* **2014**, *114*, 11619–11635.
[38] W. Liu, X. Zhang, C. Li, K. Wang, X. Sun, Y. Ma, *Chin. Chem. Lett.* **2020**, *31*, 2225–2229.
[39] Y. Wang, Y. Song, Y. Xia, *Chem. Soc. Rev.* **2016**, *45*, 5925–5950.
[40] Z. Lin, E. Goikolea, A. Balducci, K. Naoi, P. L. Taberna, M. Salanne, G. Yushin, P. Simon, *Mater. Today* **2018**, *21*, 419–436.
[41] T. Du, Z. Liu, X. Sun, L. Geng, X. Zhang, Y. An, X. Zhang, K. Wang, Y. Ma, *J. Power Sources* **2020**, *478*, 228994.
[42] X. Yu, M. Shao, X. Yang, C. Li, T. Li, D. Li, R. Wang, L. Yin, *Chin. Chem. Lett.* **2020**, *31*, 2215–2218.
[43] H. Kim, M.-Y. Cho, M.-H. Kim, K.-Y. Park, H. Gwon, Y. Lee, K. C. Roh, K. Kang, *Adv. Energy Mater.* **2013**, *3*, 1500–1506.
[44] Q. Zhou, M. Tian, Z. Ying, Y. Dan, F. Tang, J. Zhang, J. Zhu, X. Zhu, *Electrochem. Commun.* **2020**, *111*, 106663.

[45] L. Ye, Q. Liang, Y. Lei, X. Yu, C. Han, W. Shen, Z.-H. Huang, F. Kang, Q.-H. Yang, *J. Power Sources* **2015**, *282*, 174–178.
[46] X. Zhou, L. Yu, X. W. Lou, *Adv. Energy Mater.* **2016**, *6*, 1600451.
[47] P. Zhang, Q. Z. Zhu, Z. R. X. Guan, Q. Zhao, N. Sun, B. Xu, *ChemSusChem* **2020**, *13*, 1621–1628.
[48] S. Zhang, C. Li, X. Zhang, X. Sun, K. Wang, Y. Ma, *ACS Appl. Mater. Interfaces* **2017**, *9*, 17136–17144.
[49] Z. Chen, H. Li, X. Lu, L. Wu, J. Jiang, S. Jiang, J. Wang, H. Dou, X. Zhang, *ChemElectroChem* **2018**, *5*, 1516–1524.
[50] Z. Hu, Q. He, Z. Liu, X. Liu, M. Qin, B. Wen, W. Shi, Y. Zhao, Q. Li, L. Mai, *Sci. Bull.* **2020**, *65*, 1154–1162.
[51] X. Zhao, X. Zhang, C. Li, X. Sun, J. Liu, K. Wang, Y. Ma, *ACS Sustainable Chem. Eng.* **2019**, *7*, 11275–11283.
[52] W.-L. Xie, X.-D. Zhang, W.-H. Liu, Q. Xie, G.-W. Wen, X.-X. Huang, J.-D. Zhu, F.-X. Ma, *Rare Met.* **2019**, *38*, 206–209.
[53] X. Ye, Z. Lin, S. Liang, X. Huang, X. Qiu, Y. Qiu, X. Liu, D. Xie, H. Deng, X. Xiong, Z. Lin, *Nano Lett.* **2019**, *19*, 1860–1866.
[54] B.-P. Wang, R. Lv, D.-S. Lan, *Rare Met.* **2019**, *38*, 996–1002.
[55] G. Jeong, Y.-U. Kim, H. Kim, Y.-J. Kim, H.-J. Sohn, *Energy Environ. Sci.* **2011**, *4*, 1986–2002.
[56] R. Hou, B. Liu, Y. Sun, L. Liu, J. Meng, M. D. Levi, H. Ji, X. Yan, *Nano Energy* **2020**, *72*, 104728.
[57] H. Kang, Y. Liu, K. Cao, Y. Zhao, L. Jiao, Y. Wang, H. Yuan, *J. Mater. Chem. A* **2015**, *3*, 17899–17913.
[58] L. L. Zhang, X. S. Zhao, *Chem. Soc. Rev.* **2009**, *38*, 2520–2531.
[59] Y. Ma, H. Chang, M. Zhang, Y. Chen, *Adv. Mater.* **2015**, *27*, 5296–5308.
[60] H. Hu, M. Wu, *J. Mater. Chem. A* **2020**, *8*, 7066–7082.
[61] J. M. Campillo-Robles, X. Artetxe, K. del Teso Sánchez, C. Gutiérrez, H. Macicior, S. Röser, R. Wagner, M. Winter, *J. Power Sources* **2019**, *425*, 110–120.
[62] T. Peng, Z. Tan, M. Zhang, L. Li, Y. Wang, L. Guan, X. Tan, L. Pan, H. Fang, M. Wu, *Carbon* **2020**, *165*, 296–305.
[63] W. Shao, F. Hu, C. Song, J. Wang, C. Liu, Z. Weng, X. Jian, *J. Mater. Chem. A* **2019**, *7*, 6363–6373.
[64] X. Wu, Y. Chen, Z. Xing, C. W. K. Lam, S. S. Pang, W. Zhang, Z. Ju, *Adv. Energy Mater.* **2019**, *38, 1900343*.
[65] C. Li, X. Zhang, C. Sun, K. Wang, X. Sun, Y. Ma, *J. Phys. D* **2019**, *52*, 143001.
[66] F. Su, X. Hou, J. Qin, Z. S. Wu, *Batteries & Supercaps* **2019**, *3*, 10–29.
[67] A. Jain, R. Balasubramanian, M. P. Srinivasan, *Chem. Eng. J.* **2016**, *283*, 789–805.
[68] M. A. Yahya, Z. Al-Qodah, C. W. Z. Ngah, *Renewable Sustainable Energy Rev.* **2015**, *46*, 218–235.
[69] A. Jain, V. Aravindan, S. Jayaraman, P. S. Kumar, R. Balasubramanian, S. Ramakrishna, S. Madhavi, M. P. Srinivasan, *Sci. Rep.* **2013**, *3*, 3002.
[70] S. Dsoke, B. Fuchs, E. Gucciardi, M. Wohlfahrt-Mehrens, *J. Power Sources* **2015**, *282*, 385–393.
[71] B. Li, F. Dai, Q. Xiao, L. Yang, J. Shen, C. Zhang, M. Cai, *Energy Environ. Sci.* **2016**, *9*, 102–106.
[72] B. Li, F. Dai, Q. Xiao, L. Yang, J. Shen, C. Zhang, M. Cai, *Adv. Energy Mater.* **2016**, *6*, 1600802.
[73] J. Yan, Q. Wang, T. Wei, Z. Fan, *Adv. Energy Mater.* **2014**, *4*, 1300816.
[74] J. Han, H. Li, D. Kong, C. Zhang, Y. Tao, H. Li, Q.-H. Yang, L. Chen, *ACS Energy Lett.* **2020**, *5*, 1986–1995.
[75] S. Sun, F. Han, X. Wu, Z. Fan, *Chin. Chem. Lett.* **2020**, *31*, 2235–2238.
[76] Z. Yang, H. Guo, X. Li, Z. Wang, Z. Yan, Y. Wang, *J. Power Sources* **2016**, *329*, 339–346.
[77] Q. Lu, B. Lu, M. Chen, X. Wang, T. Xing, M. Liu, X. Wang, *J. Power Sources* **2018**, *398*, 128–136.
[78] Y. B. Tan, J.-M. Lee, *J. Mater. Chem. A* **2013**, *1*, 14814–14843.
[79] H. Nishihara, T. Kyotani, *Adv. Mater.* **2012**, *24*, 4473–4498.
[80] Y. Zhai, Y. Dou, D. Zhao, P. F. Fulvio, R. T. Mayes, S. Dai, *Adv. Mater.* **2011**, *23*, 4828–4850.
[81] H. Itoi, H. Nishihara, T. Kogure, T. Kyotani, *J. Am. Chem. Soc.* **2011**, *133*, 1165–1167.
[82] R. Shi, C. Han, H. Li, L. Xu, T. Zhang, J. Li, Z. Lin, C.-P. Wong, F. Kang, B. Li, *J. Mater. Chem. A* **2018**, *6*, 17057–17066.
[83] X. Song, X. Ma, Z. Yu, G. Ning, Y. Li, Y. Sun, *ChemElectroChem* **2018**, *5*, 1474–1483.
[84] H.-Y. Cheng, P.-Y. Cheng, X.-F. Chuah, C.-L. Huang, C.-T. Hsieh, J. Yu, C.-H. Lin, S.-Y. Lu, *Chem. Eng. J.* **2019**, *374*, 201–210.
[85] A. Banerjee, K. K. Upadhyay, D. Puthusseri, V. Aravindan, S. Madhavi, S. Ogale, *Nanoscale* **2014**, *6*, 4387–4394.
[86] K. Zou, P. Cai, B. Wang, C. Liu, J. Li, T. Qiu, G. Zou, H. Hou, X. Ji, *Nano-Micro Lett.* **2020**, *12*, 121.
[87] M. F. El-Kady, Y. Shao, R. B. Kaner, *Nat. Rev. Mater.* **2016**, *1*, 16033.
[88] D. X. Luong, K. V. Bets, W. A. Algozeeb, M. G. Stanford, C. Kittrell, W. Chen, R. V. Salvatierra, M. Ren, E. A. McHugh, P. A. Advincula, Z. Wang, M. Bhatt, H. Guo, V. Mancevski, R. Shahsavari, B. I. Yakobson, J. M. Tour, *Nature* **2020**, *577*, 647–651.
[89] M. Velicky, D. F. Bradley, A. J. Cooper, E. W. Hill, I. A. Kinloch, A. Mishchenko, K. S. Novoselov, H. V. Patten, P. S. Toth, A. T. Valota, S. D. Worrall, R. A. W. Dryfe, *ACS Nano* **2014**, *8*, 10089–10100.
[90] K. S. Novoselov, A. K. Geim, S. V. Morozov, D. Jiang, Y. Zhang, S. V. Dubonos, I. V. Grigorieva, A. A. Firsov, *Science* **2004**, *306*, 666–669.
[91] F. Bonaccorso, L. Colombo, G. Yu, M. Stoller, V. Tozzini, A. C. Ferrari, R. S. Ruoff, V. Pellegrini, *Science* **2015**, *347*, 1246501.
[92] M. Zeng, W.-L. Wang, X.-D. Bai, *Chin. Phys.* **2013**, *22*, 098105.
[93] X. Yao, Y. Zhao, *Chem* **2017**, *2*, 171–200.
[94] H. Banda, S. Perie, B. Daffos, P.-L. Taberna, L. Dubois, O. Crosnier, P. Simon, D. Lee, G. De Paepe, F. Duclairoir, *ACS Nano* **2019**, *13*, 1443–1453.
[95] X. Yang, C. Cheng, Y. Wang, L. Qiu, D. Li, *Science* **2013**, *341*, 534–537.
[96] Y. Zhu, S. Murali, M. D. Stoller, K. Ganesh, W. Cai, P. J. Ferreira, A. Pirkle, R. M. Wallace, K. A. Cychosz, M. Thommes, *Science* **2011**, *332*, 1537–1541.
[97] W.-Y. Tsai, R. Lin, S. Murali, L. L. Zhang, J. K. McDonough, R. S. Ruoff, P.-L. Taberna, Y. Gogotsi, P. Simon, *Nano Energy* **2013**, *2*, 403–411.
[98] J. H. Lee, W. H. Shin, M. H. Ryou, J. K. Jin, J. Kim, J. W. Choi, *ChemSusChem* **2012**, *5*, 2328–2333.
[99] V. Aravindan, D. Mhamane, W. C. Ling, S. Ogale, S. Madhavi, *ChemSusChem* **2013**, *6*, 2240–2244.
[100] M. D. Stoller, S. Murali, N. Quarles, Y. Zhu, J. R. Potts, X. Zhu, H. W. Ha, R. S. Ruoff, *Phys. Chem. Chem. Phys.* **2012**, *14*, 3388–3391.
[101] D. Mhamane, V. Aravindan, M.-S. Kim, H.-K. Kim, K. C. Roh, D. Ruan, S. H. Lee, M. Srinivasan, K.-B. Kim, *J. Mater. Chem. A* **2016**, *4*, 5578–5591.
[102] H. Wang, C. Guan, X. Wang, H. J. Fan, *Small* **2015**, *11*, 1470–1477.
[103] F. Zhang, T. Zhang, X. Yang, L. Zhang, K. Leng, Y. Huang, Y. Chen, *Energy Environ. Sci.* **2013**, *6*, 1623–1632.
[104] H. Shao, Y. C. Wu, Z. Lin, P. L. Taberna, P. Simon, *Chem. Soc. Rev.* **2020**, *49*, 3005–3039.
[105] L. A. Jurado, R. M. Espinosa-Marzal, *Sci. Rep.* **2017**, *7*, 4225.
[106] X. Zhao, C. Johnston, P. S. Grant, *J. Mater. Chem.* **2009**, *19*, 8755–8760.
[107] R. Shi, C. Han, X. Xu, X. Qin, L. Xu, H. Li, J. Li, C. P. Wong, B. Li, *Chem. Eur. J.* **2018**, *24*, 10460–10467.
[108] Y. Hao, S. Wang, Y. Shao, Y. Wu, S. Miao, *Adv. Energy Mater.* **2019**, *10, 1902836*.
[109] M. Yang, Y. Zhong, J. Ren, X. Zhou, J. Wei, Z. Zhou, *Adv. Energy Mater.* **2015**, *5*, 1500550.
[110] W. S. V. Lee, E. Peng, M. Li, X. Huang, J. M. Xue, *Nano Energy* **2016**, *27*, 202–212.
[111] T. Rauhala, J. Leis, T. Kallio, K. Vuorilehto, *J. Power Sources* **2016**, *331*, 156–166.
[112] D. Tie, S. Huang, J. Wang, J. Ma, J. Zhang, Y. Zhao, *Energy Storage Mater.* **2019**, *21*, 22–40.
[113] R. V. Salvatierra, D. Zakhidov, J. Sha, N. D. Kim, S. K. Lee, A. O. Raji, N. Zhao, J. M. Tour, *ACS Nano* **2017**, *11*, 2724–2733.
[114] Y. Sun, J. Tang, F. Qin, J. Yuan, K. Zhang, J. Li, D.-M. Zhu, L.-C. Qin, *J. Mater. Chem. A* **2017**, *5*, 13601–13609.
[115] W. Liu, J. Li, K. Feng, A. Sy, Y. Liu, L. Lim, G. Lui, R. Tjandra, L. Rasenthiram, G. Chiu, A. Yu, *ACS Appl. Mater. Interfaces* **2016**, *8*, 25941–25953.
[116] N.-W. Li, X. Du, J.-L. Shi, X. Zhang, W. Fan, J. Wang, S. Zhao, Y. Liu, W. Xu, M. Li, Y.-G. Guo, C. Li, *Electrochim. Acta* **2018**, *281*, 459–465.
[117] M. Arnaiz, D. Shanmukaraj, D. Carriazo, D. Bhattacharjya, A. Villaverde, M. Armand, J. Ajuria, *Energy Environ. Sci.* **2020**, *13*, 2441–2449.
[118] L. Jin, C. Shen, A. Shellikeri, Q. Wu, J. Zheng, P. Andrei, J.-G. Zhang, J. P. Zheng, *Energy Environ. Sci.* **2020**, *13*, 2341–2362.
[119] C. Sun, X. Zhang, C. Li, K. Wang, X. Sun, Y. Ma, *Energy Storage Mater.* **2020**, *32*, 497–516.
[120] H. Shi, J. Barker, M. Y. Saidi, R. Koksbang, L. Morris, *J. Power Sources* **1997**, *68*, 291–295.
[121] J. R. Dahn, T. Zheng, Y. H. Liu, J. S. Xue, *Science* **1995**, *270*, 590–593.
[122] Y. Nishi, *Chem. Rec.* **2001**, *1*, 406–413.
[123] M. Winter, J. O. Besenhard, M. E. Spahr, P. Novak, *Adv. Mater.* **1998**, *10*, 725–763.
[124] S. S. Zhang, *J. Electrochem. Soc.* **2020**, *167*, 100510.
[125] S. R. Sivakkumar, A. S. Milev, A. G. Pandolfo, *Electrochim. Acta* **2011**, *56*, 9700–9706.

[126] M. L. Divya, S. Natarajan, Y.-S. Lee, V. Aravindan, *J. Mater. Chem. A* **2020**, *8*, 4950–4959.
[127] S. Jayaraman, G. Singh, S. Madhavi, V. Aravindan, *Carbon* **2018**, *134*, 9–14.
[128] S. Jayaraman, S. Madhavi, V. Aravindan, *J. Mater. Chem. A* **2018**, *6*, 3242–3248.
[129] Z. Yang, H. Guo, X. Li, Z. Wang, J. Wang, Y. Wang, Z. Yan, D. Zhang, *J. Mater. Chem. A* **2017**, *5*, 15302–15309.
[130] V. Khomenko, E. Raymundo-Pinero, F. Beguin, *J. Power Sources* **2008**, *177*, 643–651.
[131] M. Cai, X. Sun, W. Chen, Z. Qiu, L. Chen, X. Li, J. Wang, Z. Liu, Y. Nie, *J. Mater. Sci.* **2017**, *53*, 749–758.
[132] Z. Chen, Y. Liu, Y. Zhang, F. Shen, G. Yang, L. Wang, X. Zhang, Y. He, L. Luo, S. Deng, *Mater. Lett.* **2018**, *229*, 134–137.
[133] Y.-Q. Dai, G.-C. Li, X.-H. Li, H.-J. Guo, Z.-X. Wang, G.-C. Yan, J.-X. Wang, *Rare Met.* **2020**, *39*, 1364–1373.
[134] X. Zhou, F. Chen, T. Bai, B. Long, Q. Liao, Y. Ren, J. Yang, *Green Chem.* **2016**, *18*, 2078–2088.
[135] D. Zhai, H. Du, B. Li, Y. Zhu, F. Kang, *Carbon* **2011**, *49*, 725–729.
[136] J. Luis Gomez-Urbano, G. Moreno-Fernandez, M. Arnaiz, J. Ajuria, T. Rojo, D. Carriazo, *Carbon* **2020**, *162*, 273–282.
[137] N. Nitta, F. Wu, J. T. Lee, G. Yushin, *Mater. Today* **2015**, *18*, 252–264.
[138] J.-H. Kim, J.-S. Kim, Y.-G. Lim, J.-G. Lee, Y.-J. Kim, *J. Power Sources* **2011**, *196*, 10490–10495.
[139] J. Zhang, X. Liu, J. Wang, J. Shi, Z. Shi, *Electrochim. Acta* **2016**, *187*, 134–142.
[140] R. Fu, Z. Chang, C. Shen, H. Guo, H. Huang, Y. Xia, Z. Liu, *Electrochim. Acta* **2018**, *260*, 430–438.
[141] W. J. Cao, J. P. Zheng, *J. Power Sources* **2012**, *213*, 180–185.
[142] W. J. Cao, J. F. Luo, J. Yan, X. J. Chen, W. Brandt, M. Warfield, D. Lewis, S. R. Yturriaga, D. G. Moye, J. P. Zheng, *J. Electrochem. Soc.* **2017**, *164*, A93–A98.
[143] W. Luo, Z. Jian, Z. Xing, W. Wang, C. Bommier, M. M. Lerner, X. Ji, *ACS Cent. Sci.* **2015**, *1*, 516–522.
[144] J. Zhang, Z. Shi, C. Wang, *Electrochim. Acta* **2014**, *125*, 22–28.
[145] M. Schroeder, S. Menne, J. Ségalini, D. Saurel, M. Casas-Cabanas, S. Passerini, M. Winter, A. Balducci, *J. Power Sources* **2014**, *266*, 250–258.
[146] Z. Li, X. Sun, W. Liu, X. Zhang, K. Wang, Y. Ma, *J. Electrochem.* **2019**, *25*, 122–136.
[147] Y.-G. Lim, M.-S. Park, K. J. Kim, K.-S. Jung, J. H. Kim, M. Shahabuddin, D. Byun, J.-S. Yu, *J. Power Sources* **2015**, *299*, 49–56.
[148] M. Schroeder, M. Winter, S. Passerini, A. Balducci, *J. Power Sources* **2013**, *238*, 388–394.
[149] Y. H. Liu, J. S. Xue, T. Zheng, J. R. Dahn, *Carbon* **1996**, *34*, 193–200.
[150] R. Raccichini, A. Varzi, S. Passerini, B. Scrosati, *Nat. Mater.* **2015**, *14*, 271–279.
[151] Z.-S. Wu, G. Zhou, L.-C. Yin, W. Ren, F. Li, H.-M. Cheng, *Nano Energy* **2012**, *1*, 107–131.
[152] Q. Zhao, J. Liu, X. Li, Z. Xia, Q. Zhang, M. Zhou, W. Tian, M. Wang, H. Hu, Z. Li, W. Wu, H. Ning, M. Wu, *Chem. Eng. J.* **2019**, *369*, 215–222.
[153] J. J. Ren, L. W. Su, X. Qin, M. Yang, J. P. Wei, Z. Zhou, P. W. Shen, *J. Power Sources* **2014**, *264*, 108–113.
[154] W. Ahn, D. U. Lee, G. Li, K. Feng, X. Wang, A. Yu, G. Lui, Z. Chen, *ACS Appl. Mater. Interfaces* **2016**, *8*, 25297–25305.
[155] C. Li, X. Zhang, K. Wang, X. Sun, Y. Ma, *Carbon* **2018**, *140*, 237–248.
[156] Y. Luan, R. Hu, Y. Fang, K. Zhu, K. Cheng, J. Yan, K. Ye, G. Wang, D. Cao, *Nano-Micro Lett.* **2019**, *11*, 1–13.
[157] R. Tjandra, W. Liu, L. Lim, A. Yu, *Carbon* **2018**, *129*, 152–158.
[158] Y. Kim, S. C. Woo, C. S. Lee, J. S. Park, H. Seo, J.-H. Kim, J. H. Song, *J. Electroanal. Chem.* **2020**, *863*, 114060.
[159] Q. Xia, H. Yang, M. Wang, M. Yang, Q. Guo, L. Wan, H. Xia, Y. Yu, *Adv. Energy Mater.* **2017**, *7*, 1701336.
[160] M. Liu, Z. Zhang, M. Dou, Z. Li, F. Wang, *Carbon* **2019**, *151*, 28–35.
[161] D. P. Dubal, P. Gomez-Romero, *Mater. Today Energy* **2018**, *8*, 109–117.
[162] J. Jiang, J. Yuan, P. Nie, Q. Zhu, C. Chen, W. He, T. Zhang, H. Dou, X. Zhang, *J. Mater. Chem. A* **2020**, *8*, 3956–3966.

Manuscript received: November 5, 2020
Revised manuscript received: December 9, 2020
Accepted manuscript online: December 10, 2020
Version of record online: January 4, 2021